



Recent Control Technologies for Floating Offshore Wind Energy System: A Review

Kwangtae Ha¹ · Hoai Vu Anh Truong² · Tri Dung Dang^{2,3} · Kyoung Kwan Ahn²

Received: 17 June 2020 / Revised: 20 August 2020 / Accepted: 7 September 2020 / Published online: 6 October 2020
© Korean Society for Precision Engineering 2020

Abstract

This paper presents the recent control technologies being researched for floating offshore wind energy system (FOWES). FOWES has been getting many attentions recently as an alternative energy system utilizing vast sustainable wind resource away from land with little restriction by human societies, artificial and natural obstacles. However, not only due to the harsh environmental conditions such as strong wind, wave, and current, but also due to the platform motions such as surge, sway, heave, pitch, roll, and yaw, there could occur many problems including less energy capture than expected, frequent emergency stops, turbine structural instability, and fatigues resulting in early failures, which stay the levelized cost of energy (LCOE) still high compared to conventional fixed offshore wind energy system. These risks could be lowered by operating the turbine close to the optimum point and harvesting wind energy efficiently even under strong wind conditions with the properly applied control technologies, while reducing the loads on structural components. Many researches have been actively going on not only by numerical approaches, but also by experimental tests. This study is wrapping the most recent researches on control technologies for promising floating offshore wind energy system according to different substructure designs such as a spar type, semi-submersible type, tension-leg platform (TLP) type, and barge type, and discusses about its challenges as well.

Keywords Green technology · Floating offshore wind energy system (FOWES) · Substructures · Control algorithm · Individual pitch control (IPC) · Collective pitch control (CPC)

Abbreviations

OWT	Offshore wind turbine
FOWT	Floating offshore wind turbine
WTG	Wind turbine generator
RNA	Rotor-nacelle assembly
LCOE	Levelized cost of energy
OPEX	Operating expenditure
CAPEX	Capital expenditure
MPPT	Maximum power point tracking
IPC	Individual pitch control
CPC	Collective pitch control

1 Introduction

Wind energy has been in the spotlight as a major source of renewable energy, and its levelized cost of energy (LCOE) are becoming lowered through large wind farm construction and increased rotor size and capacity of wind turbines with innovative technologies as shown in Fig. 1, which lead to a preferable choice among other alternative renewable energy sources against fossil fuel energy [1–4]. With innovatively engineered designs of rotor blade airfoils and structures using recent powerful computational performance, wind turbines have been designed to extract wind energy as close as possible to the Betz limit, 59.3% [5–12]. Currently, total energy capacity of existing wind energy conversion system has grown from 23.9 in 2001 and to 591 GW in 2019, approximately 25 times increase has been achieved, and there is still a strong demand of wind power in alternative energy market, and even up to the total capacity of 1787 GW by 2030 with reduced LCOE along with improved technologies are expected [13]. Among total wind turbines, new installations of offshore wind turbines are continuously growing as shown in Fig. 2 [14].

✉ Kyoung Kwan Ahn
kkahn@ulsan.ac.kr

¹ Department of Floating Offshore Wind Energy System, University of Ulsan, 93, Deahak-Ro, Nam-Gu, Ulsan 44610, South Korea

² Department of Mechanical Engineering, University of Ulsan, 93, Deahak-Ro, Namgu, Ulsan 44610, South Korea

³ Department of Mechatronics, Ho Chi Minh City University of Technology and Education, Ho Chi Minh City 700000, Vietnam

A GROWTH IN CAPACITY

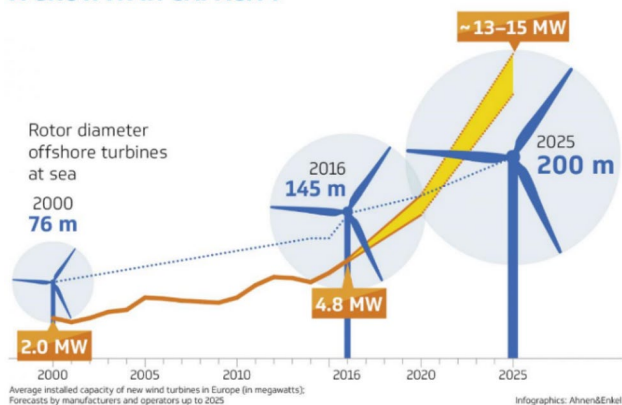


Fig. 1 Growth in rotor size and capacity of offshore wind turbine [4]

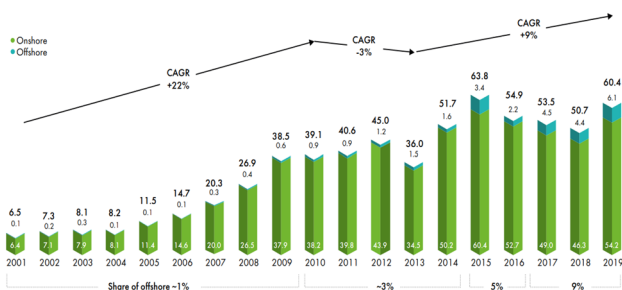


Fig. 2 Historic development of new installations (onshore and offshore) [14]

The term offshore means something like "off the coast". Offshore wind energy (OWE) system thus means the electricity production by wind turbine system either with fixed or with floating substructure types in the ocean. The advantages of OWE are that it can utilize the higher and steadier wind resource at sea with reduced wind shear due to low surface friction and no physical restriction like hills or artificial buildings [15]. Therefore, offshore wind farms can produce twice as much electricity as comparable wind plants on land, therefore, it leads to a high level of reliability in power generation [16]. Besides, since this is built at sea far away from land, it could eliminate many restrictions such as noise regulation, shadow flicker, and other society objections [17]. Therefore, offshore wind energy can make a significant contribution to the energy transition, i.e. when switching to renewable energies and moving away from nuclear power and fossil fuels.

OWT is categorized further into fixed OWT and floating OWT depending on the substructure types. Fixed offshore wind turbines can be installed normally up to 40 m with current technologies with various types of substructures. Due to installation limit up to 40~50 m water depth, however, these are not applicable to many Asian countries such

as South Korea or Japan, and other countries with limited shallow waters [18]. With development of innovative floating structures, the concept of floating offshore wind turbine (FOWT) was introduced and demonstrated first at North Sea near Norway, called Hywind Project with 2.3 MW wind turbine with a spar type floating foundation at 2009 [19]. After successful demonstration, many commercial floating offshore wind farm and projects are either operating or under development, therefore, the capacity potential of the FOWE is expected to be around 5–30 GW by 2030 as a new way of power generation [20, 21].

For a wind turbine to operate safely and produce energy from wind efficiently, the control system is necessary to link the operations of all the subsystems closely together. In early days of wind energy system, control system is just a tool to operate wind turbine sequentially. However, as the size of a wind turbine system is getting larger as previously shown in Fig. 1, control technologies become important to achieve higher energy production under harsh environments with better safety condition, and to reduce OPEX with less faulty events and health monitoring system [22]. For example, the system executes the operational sequence, monitor the status of wind turbine system, enable the safety operation such as parking brake, adjust blade pitch angle, and connect wind turbine to grids. Control technologies for fixed offshore wind turbine are similar to each other because wind turbine system is fixed at the seabed through substructures.

Unlike to fixed offshore wind turbine, floating offshore wind turbines (FOWTs) use floating substructures such as barge type, TLP type, spar type, and semi-submersible type. Because of the different buoyance principle of each type, their stability and dynamic motion heavily rely on the adequately designed control technologies in addition to the general control concept adapted to fixed offshore wind energy system [23]. For the realization of a successful floating offshore wind turbine operation, the consideration of proper control technologies depending on the floating foundations is imperative for the best performance and safety [24].

In this review paper, recent control technologies according to various floating foundations will be discussed, which is highly related to wind turbine power performance and efficiency related to LCOE. Prior to main topic, a brief explanation of floating offshore wind energy and traditional control principle will be provided to readers.

2 Floating Offshore Wind Turbine (FOWT)

2.1 Components

Wind energy system generates electricity energy by extracting kinetic energy from wind. The onshore horizontal axis wind turbine generator (HAWT) traditionally

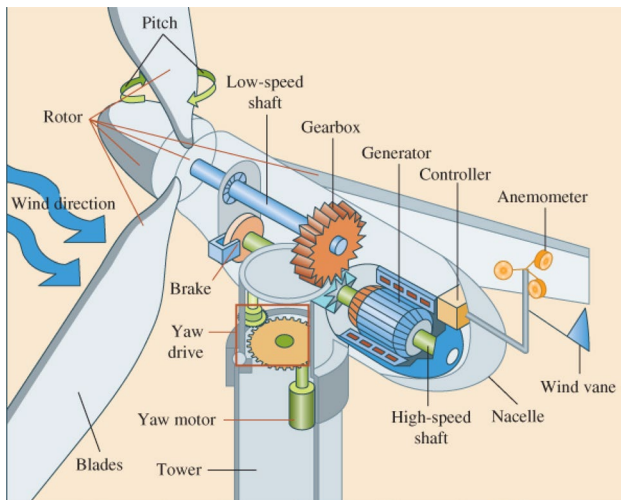


Fig. 3 A basic part of wind turbine generator [28]

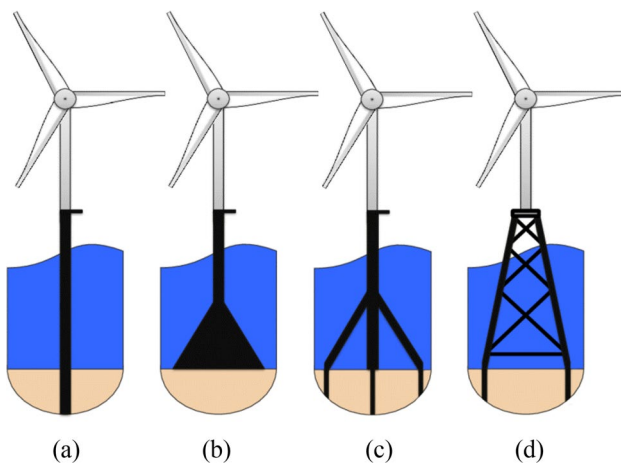


Fig. 4 Foundations of bottom-fixed offshore WES [30]: **a** monopile; **b** gravity based; **c** tripod; **d** jacket

consists of three main components, rotor including hub, nacelle system, and tower. Rotor component include single or multiple composite blades, hub, and pitch drive system (PDS), and nacelle system is composed of nacelle structure, drive train system (DTS) including low speed /high speed shafts, gear box, generator, yaw drive system (YDS), and other electronic equipment. Readers can refer to references about the functions of components in detail [25–28]. Figure 3 illustrates a basic part of wind turbine generator.

In case of offshore wind turbine generators, traditional onshore wind turbine system is connected to the bottom-fixed substructures, which include monopile, jacket, gravity-based, and tripod as shown in Fig. 4. Among them, the monopoly-type is dominant with more than 80% market share due to its low cost, easy installation, and improved

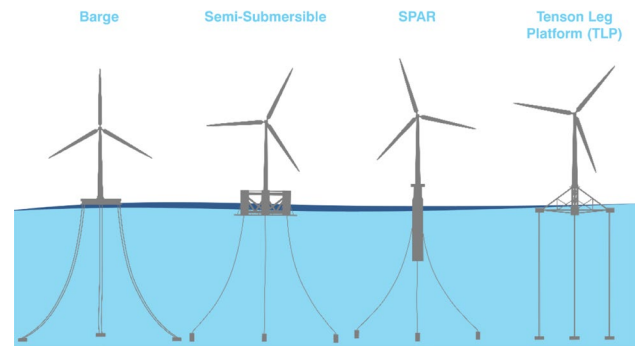


Fig. 5 Foundations of floating offshore WES [31]

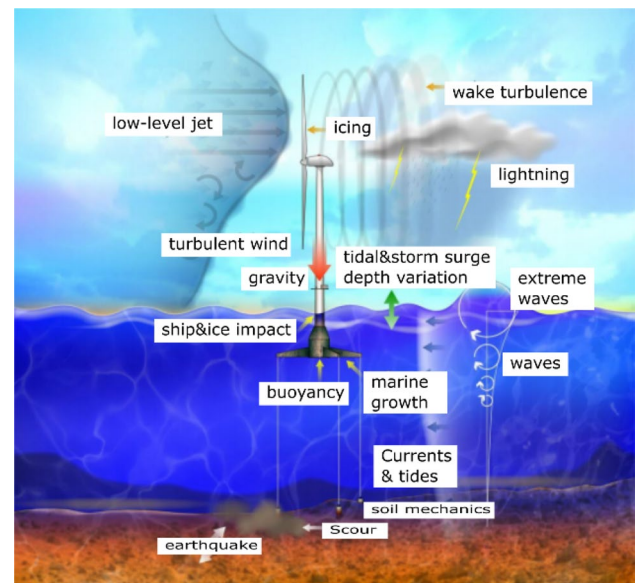


Fig. 6 Multiple loading sources of FOWT [17]

manufacturing progress related to rolling more than 10 m in diameter [29, 30].

Unlike to bottom-fixed offshore wind turbine, floating offshore wind turbines (FOWTs) consist of different types of floating foundation: Spar, Barge, TLP (Tension-Leg Platform), and Semi-submersible type as shown in Fig. 5 [31]. Other components include cable system, substation if necessary, and mooring system to secure the FOWT not to be moved away from its designated installation zone.

2.2 Loading Sources

Contrary to onshore wind energy system, offshore wind energy system either with a fixed-bottom type or with floating type, is a complex aero-hydro-servo-elastic system. Its multiple loading sources and interaction is shown in Fig. 6, and unique loads for OWT, hydrodynamic forces, are also schematically shown in Fig. 7 [17, 32–34].

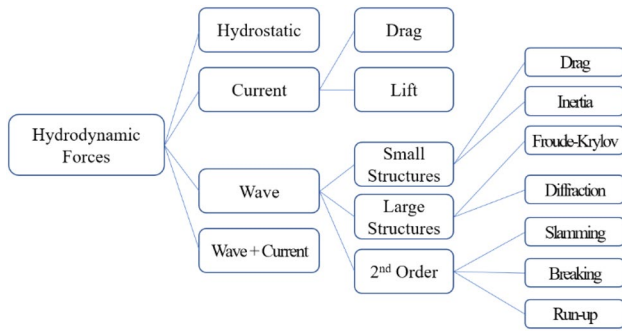


Fig. 7 Hydrodynamic forces for OWT

The loads acting on an offshore wind turbine (OWT) structure can be grouped into static and dynamic loads. Static loads are mainly related to the self-weights of the components. For example, the ice on the structure is the case of static loads due to the environment. Dynamic loads are related to the environment in the form of wind or water interaction, and classified as aerodynamic and hydrodynamic, respectively, which are the most challenging to OWT according to Yu [35]. Moreover, Tempel added that for OWTs, the assessment of environmental parameters is more extensive than for land turbines [36]. On land, turbines can be simply designed by classes prescribing the wind regime and the required resilience of the turbine itself. However, for OWTs, the winds are less turbulent but more formidable, and also the offshore environment features other actions due to the water waves and currents. This implies that engineers designing an FOWTs face a more daunting challenge and must fully understand the behavior and magnitude of the dynamic loads before proceeding with the design [37, 38]. Other loads that affect offshore structures in general include earthquakes, accidental loads, fire, and blast loading.

In other ways, multiple loading sources can also be classified as external sources and internal sources. External sources include wind, waves, sea current, gravity, ice on blades and sea, lightning, wake interaction with other turbines, earthquakes, grid related issues, etc. On the other hand, internal sources include rotating machinery, control

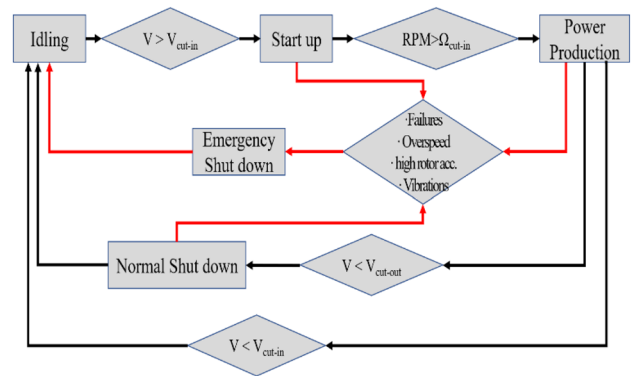


Fig. 8 Control flow in wind energy system

system, power electronics, unexpected operational faults, etc.

3 Traditional Control System for Onshore and Bottom-Fixed Offshore Wind Energy System

3.1 General Concept

A wind turbine control system comprises and ties several sensors (for example, torque, speed, accelerometers, anemometers, electrical power), actuators (for example, yaw system, pitch system) and other elements [39]. This system collects the input signals from the sensors and calculates and sets the output signals for the actuators. The controller is used to achieve the maximum power from wind, maintain safe operation of the turbine, reduce loads, and prevent faults. Main control systems used for wind turbine system are listed in Table 1.

3.2 Control Flow and Parameters

For precise performance control, sensor signal and measurement data are important, and schematic control flow of the wind turbine operating modes is shown in Fig. 8.

Table 1 Category of control system

Control category	Corresponding system
Azimuth control	Wind tracking system
Rotor speed control	Generator system
Blade angle control	Pitch system
Active power control	Converter/generator system (grid frequency support)
Reactive power control	Converter/generator system (mains voltage support)
Current and voltage control	Converter system (field-oriented control)
Temperature control	Heating devices

As shown in Fig. 8, the emergency shut down (or a quick stop) can be executed in case of failures of critical system based on the measurements (rotor speed, wind speed, currents, etc.), positioning (azimuth, pitch drive, etc.), communication network data, or generally exceeding defined threshold values. Similarly, performance reduction can be executed in case of exceeding various threshold values, which include speeds, measured forces, moments, vibration amplitudes from tower, electrical quantities (voltages and current from generator, grid or converter area), and thermal values from nacelle, drive train, or electrical system. Table 2 lists the general data type for control and monitoring of a wind turbine generator.

3.3 Control Strategy for Performance

Generally, the control objectives are dependent on the operating regions of the turbine which are related to the wind speed. Five operating regions are shown in Fig. 9.

As shown in Fig. 9, in the entire wind speed range (above a cut-in threshold), the WES is adjusted to the wind direction using the azimuth adjustment system (measured by the nacelle anemometer). The adjustment is made discontinuously at certain time intervals. In systems with power electronic converters, the DC link voltage control always sets the steady state balance between generator and grid-side active power consumption. The DC voltage of the DC link is stabilized continuously. Below the nominal wind speed, the rotor power is maximized by specifying the generator-side power as a function of the rotor speed. Above the nominal wind speed, the rotor speed is kept constant by the blade adjustment systems with a constant generator torque. The blade angle control (pitch control) usually works discontinuously at certain time intervals. Details of each operation regions are summarized in Table 3 [40].

Since electric power is produced from regions 2 to 3, two main control strategies, maximum power point tracking (MPPT) control for region 2 and blade pitch control for region 3, will be discussed in detail.

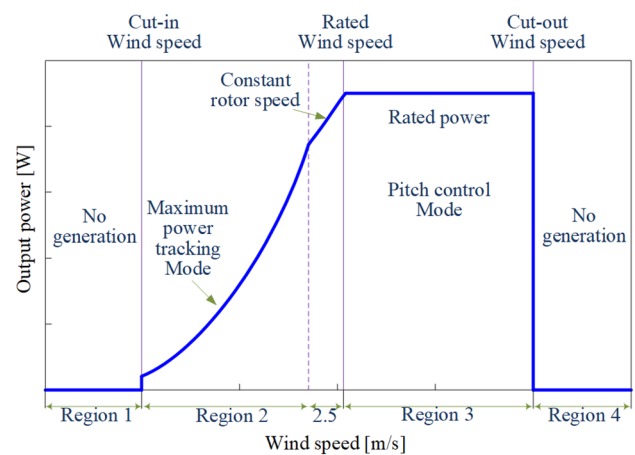


Fig. 9 Operational regions of the wind turbine based on wind speed

3.3.1 MPPT (Maximum Power Point Tracking) Control in Region 2

In region 2, the objective is to yield maximum power production via MPPT based controller such as generator torque control or speed control. Several researchers give the completed review for various control algorithms based MPPT as in [41–44]. In this region, the pitch angle should be kept at a constant optimal value (i.e. 0 degree) which can help the turbine to absorb all possible power from the wind.

The wind turbine captured power is calculated as:

$$P_{wt} = \frac{1}{2} \rho \cdot C_p(\lambda, \beta) \cdot A v_w^3 \tag{1}$$

where ρ is the air density, A is the swept area of the rotor (m^2), v_w is the wind speed (m/s) and C_p is power capture coefficient which is a function of tip speed ratio λ and pitch angle β as [45, 46]:

$$C_p(\lambda, \beta) = C_1 \left(\frac{C_2}{\lambda_i} - C_3 \beta - C_4 \right) e^{\frac{C_5}{\lambda_i}} + C_6 \lambda_i \tag{2}$$

with

Table 2 General data type and source for control and monitoring

Type	Source
Temperatures	Bearings, oil, air, converter, generator, transformer, auxiliary drives, etc.
Acceleration	Tower, nacelle, etc.
Mechanical loads	Material strains—blades, tower, mechanical drive train, etc.
General Speeds, location, position, directions	Rotor, blades, wind, generator, nacelle, etc.
Transmission/hydraulic status data	Oil status—water/particle content, fill levels, pressure, etc.
Basic electrical quantities	Currents, voltages in the generator, converter, mains and auxiliary drives, control, etc.
General condition data	Ice formation, moisture, condensation, filter contamination, vibrations, noise, feather mouse detector, aircraft approach, etc.

Table 3 Basic control strategy at each operational region

Region	Description
1	Region 1 has the wind speed lower than the limit required for the turbine to rotate and there is no power production, the turbine should be kept idle
2	Once the wind speed exceeds, the rotor starts to rotate and enters region 2 which is bounded between cut-in and just below the rated wind speed. In this region, the power of the wind increases progressively as the wind speed increases. Turbine torque and speed control based MPPT are required to maximize output power. Pitch angle should be kept at an optimal value
2.5	To obtain a smooth transition from Region 2 to Region 3, closed loop torque control is used to achieve constant rotor speed, where the blade pitch angle is fixed
3	Region 3 is placed between the rated and the cut-out wind speeds, the output power of the turbine must be limited to the rated value. The pitch angle needs to be controlled to maintain the rated generator power to limit the generator speed and mechanical loads
4	The wind turbine must have a mechanical brake to switch off due to high wind gusts

$$P_{wt} = \frac{1}{2} \rho \cdot C_p(\lambda, \beta) \cdot Av_w^3 \tag{3}$$

$$\frac{1}{\lambda_i} = \frac{1}{\lambda + 0.08\beta} - \frac{0.035}{\beta^3 + 1} \tag{4}$$

where the coefficients $C_1 \sim C_6$ are different for different rotors, i.e. for a particular NREL 5 MW wind turbine rotor the coefficients are: $C_1=0.5176$, $C_2=116$, $C_3=0.4$, $C_4=5$, $C_5=21$ and $C_6=0.0068$ [45, 46]. The tip speed ratio of the wind turbine λ is as following:

$$\lambda = \frac{\omega_r \cdot R}{v_w} \tag{5}$$

where R is the rotor radius (m), ω_r is the rotor angular velocity (rad/s).

According to the wind speed, there exists a specific rotor speed ω_r that extracts maximum power (optimal tip speed ratio λ_{opt}) as shown in Fig. 10 [45, 46]. The generator torque must be adjusted to accelerate or decelerate the turbine rotor by the controller to obtain the optimum power coefficient $C_{p,opt}$ at λ_{opt} .

Tip speed ratio (TSR) based MPPT controller keeps the ratio between the speed of the tip of the blade and wind speed to an optimum value. TSR based MPPT requires the feedback of the rotor speed to adjust it to the desired value. Figure 11 shows the diagram of the TSR based MPPT. This method is efficient with a fast response. It is simple but it requires the knowledge of the wind speed via anemometers which are very sensitive due to downwind wake. Some control algorithm can be applied to reduce the error between the rotor speed and its optimal value, such as adaptive fuzzy sliding mode controller AFSMC [45, 46], Proportional-integral PI controller [47], Proportional-integral-derivative PID controller [48, 49], adaptive neuro-fuzzy inference system ANFIS [50].

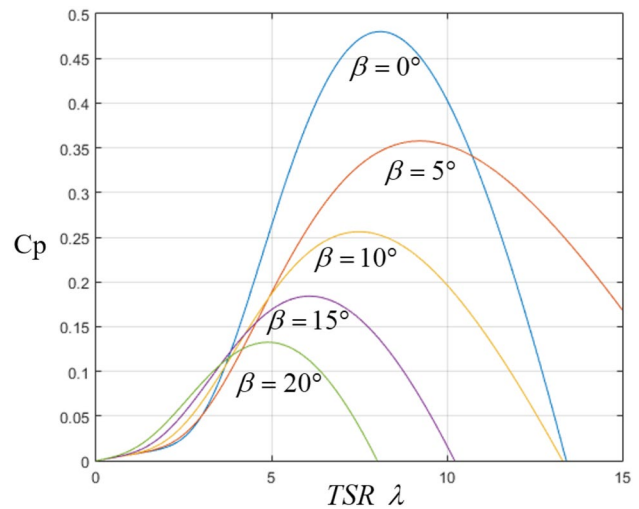


Fig. 10 Power coefficient related to TSR and pitch angle [45, 46]

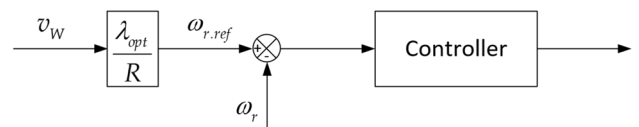


Fig. 11 TSR based MPPT control diagram. Reproduced with permission from [42]. Copyright 2016, Elsevier

Optimal torque (OT) based MPPT adjusts the generator torque to the desired torque of maximum power. The optimal torque can be calculated as:

$$T_{gopt} = k_{opt} \omega_r^2 \tag{6}$$

$$k_{opt} = \frac{1}{2} \rho \pi R^5 \frac{C_{p,opt}}{\lambda_{opt}^3}, \tag{7}$$

where k_{opt} is constant from the aerodynamic characteristics of each WT, ω_r is rotor speed, ρ is the air density, R is the

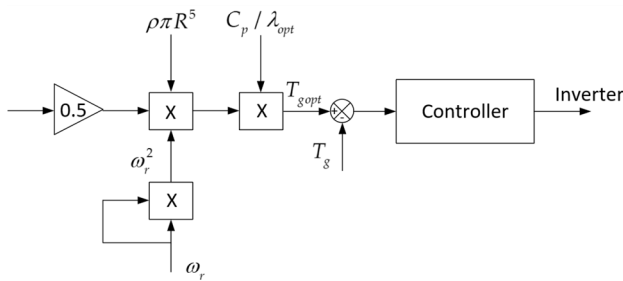


Fig. 12 OT based MPPT control diagram. Reproduced with permission from [42]. Copyright 2016, Elsevier

rotor radius, $C_{p,opt}$ is the optimum power coefficient and λ_{opt} is optimal tip speed ratio.

Wind speed information is not required in this method. However, it requires the mechanical parameters of the turbine which are difficult to obtain for individual WT. Furthermore, the OT curve will change over time after the operation. Figure 12 shows the diagram of the OT based MPPT. The controllers only require the shaft speed input, which is easy to obtain using speed sensors. Some researchers applied control algorithms to increase the accuracy of the control system such as PI [51–53], H_∞ loop shaping [54], fuzzy integral sliding mode [55], fuzzy logic control [56], adaptive integral sliding mode with a recurrent neural network to identify the uncertain wind turbine dynamics [57].

3.3.2 Blade pitch control in region 3

In region 3, the pitch angle needs to be systematically manipulated to maintain the rated generator power. The goals of pitch control are to save the turbine from overload resulted from the sudden wind gust, maximize the generated power under normal operation [44, 58]. There are two types of pitch control system actuators which are electrotechnical pitch actuator and hydraulic pitch actuator [59, 60]. The pitch control turns the blades around their axes to increase or decrease the relative wind flow and to avoid aerodynamic overloads on the rotor while keeping the rated power. Figure 13 shows the structures of pitch angle control strategies according to three different input signals. In Fig. 13a, the pitch angle–wind speed curve is applied to obtain the pitch angle reference for specific wind speed. This is the simplest control strategy but not an appropriate one since it is difficult to precisely measure the wind speed. In Fig. 13b, the generator speed reference is compared to its measured value. The controller receives the error to produce the pitch angle reference. In Fig. 13c, the generator power—the generator power reference is compared to its measured value. The controller receives the error to produce the pitch angle reference. Usually, an adaptive/tuning concept is added to this type due

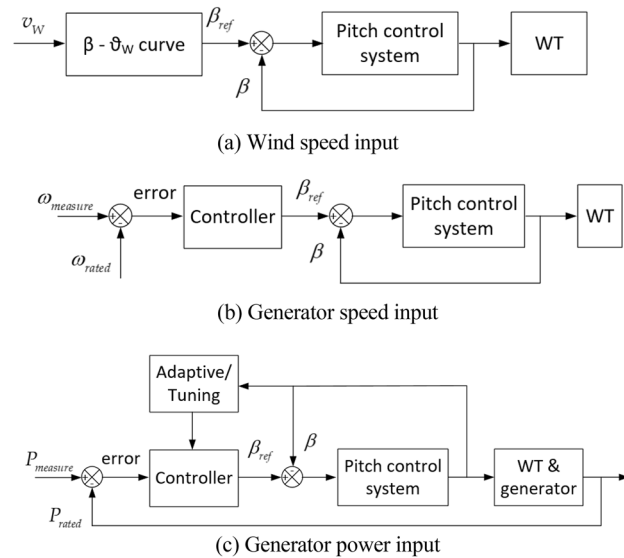


Fig. 13 Blade pitch angle control strategies based on input signals. Reproduced with permission from [44]. **a** Windspeed input, **b** generator speed input, **c** generator power input. Copyright 2016, Elsevier

to the very small sensitivity of aerodynamic torque to pitch angle. Hence, it requires a larger gain at high wind speeds.

PI controller [61–66] or PID controller [67, 68] is usually used since they are simple and robust. Other methods based on adaptive concepts to compensate for the uncertainties or disturbance as in [69–73]. The combination often includes sliding mode control [69–71, 73–75], back-stepping technique [70, 72], fuzzy logic control [69, 71, 75, 76] to enhance the control performance. Neural network can also be used for the predictive problem of the pitch angle [77].

The collective pitch control (CPC) and individual pitch control (IPC) are widely used blade pitch control schemes, where CPC technique means that the pitch commanded value is the same for all blades, and individual pitch control (IPC) has the specific goal of load reduction where the pitch angle reference values are different on each blade [63, 64, 66, 76, 78]. In the following section, current control technologies researched for FOWT to stabilize the motion while maximizing power performance are reviewed which include CPC, IPC, and hybrid IPC-CPC strategy.

4 Advanced Control Technologies for Floating Offshore Wind Turbines (FOWT) with Various Substructure Types

Implementing control algorithms for the FOWT is more complicated than land-based wind turbines not only due to the influences from multiple loading as previously shown in Fig. 6 in section, but also due to the stabilization method as shown in Fig. 14 [79].

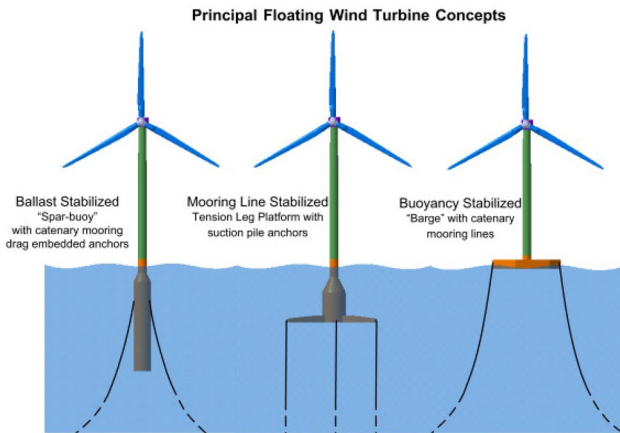


Fig. 14 Stability approach for various substructures of a FOWT [79]

In this section, control technologies developed specifically for four different substructure types of FOWT will be explained in detail.

4.1 Control for FOWT with Barge Type (B-FOWT)

The configuration of FOWT with barge type (B-FOWT) was shown in Fig. 14. This structure is erected with a waterplane stabilized platform and constrained by mooring wires.

Investigated operation under high wind speed and aimed to regulate the pitch and generator torque, Bagherieh et al. [80] studied and verified their suggested algorithm on the model of 5-MW B-FOWT with the use of FAST model. For simplicity, the author systematically linearized the dynamics model with a linear parameter-varying (LPV) method. Subsequently, an output state feedback based on linear quadratic regulator (LQR) gain-scheduling (GS) and LPV-GS are preferred to examine and compare with traditional gain-scheduling (GS), gain-scheduling-proportional-integral (GSPI) controller, and fixed LQR controller. The general block diagram of this controller is sketched in Fig. 15 in which Ω_g and Ω_{g_ref} are actual generator speed and reference speed, respectively; β_{eq} is equivalent blade pitch angle, T_{g_eq} is generator torque equivalent, x_{eq} is state equivalent, and u_d denotes disturbance. For the power regulation, the LQR-GS returned the best performance while the LPV-GS exported a significant reduction of platform pitching. The power regulation under LPV-GS control could be improved with suitable tuned weighting factors which can be figured from the paper results.

The idea for using the individual blade pitch control (IPC) is that each blade is adjusted separately to keep the platform balance. In particularly, when the platform rotates forward, the blade at the top-half section of the rotor hub is controlled to increase the thrust action and the other two bottom blades are controlled to reduce the thrust. These actions

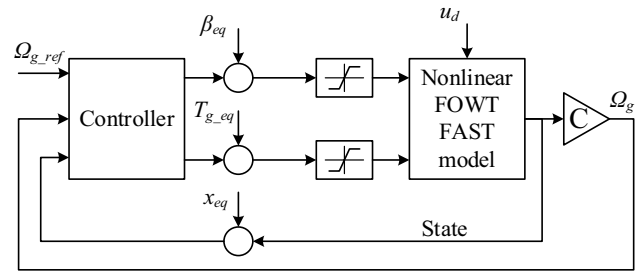


Fig. 15 Control algorithm based on state feedback and output feedback methods. Reproduced with permission from [80]. Copyright 2015, Springer Nature

yield a lowest change in rotor thrust and store backward pitching moment; thus, lowering the pitching movement of the platform.

The first applied IPC on the B-FOWT is referred to [81–84]. Namik et al. derived the comprehensive model and considered multi objectives by conducting an advanced state-space (SS) feedback control. In this contribution, the author clarified several configurations for developing advanced control methodologies over the baseline control like Multi-Input-Multi-Output (MIMO) state-space feedback control (SFC). This MIMO controller was suitable for IPC since each blade pitch is differently adjusted. Three controllers including (1) baseline collective pitch control (CPC)-PI, (2) SS-CPC based decentralized control, and (3) SS-IPC were introduced to investigate the system behavior. The block control diagram is shown in Fig. 16. The setpoints for the generator torque was changeable in comparison with previous publication with a fixed value. The simulation took a comparison between the three controllers to verify how much system improvement could be achieved on the B-FOWT under the condition of high wind speed. The simulation was implemented by using FAST model and MATLAB/Simulink program. The results indicated that the

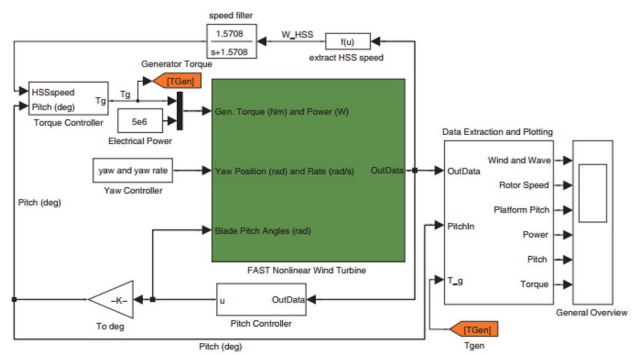


Fig. 16 IPC-based State feedback control [81–85]. Copyright 2018, American Institute of Aeronautics and Astronautics, Inc., with permission

IPC could improve up to 33% power performance and the CPC-SFC could improve up to 44%. However, the platform rolling and pitching velocity could be suppressed approximately 39% and 43% under the IPC, respectively, and 10% and 13% under controlled by the SS-CPC.

4.2 Control for FOWT with TLP type (T-FOWT)

The TLP (tension-leg platform) structure is constructed by a floating buoy and stabilized by tensioned wires in vertical which are connected to the seabed as shown in Fig. 14. These tendons are required to withstand high tension due to structure buoyancy.

In this type of FOWT, the first approach employing advanced control was reported by Betti [85]. The author proposed using a robust H_∞ controller with the use of a light detector and ranging (LIDAR) to establish a stable response of the simplified 2-D TLP model at the rated speed. Besides, the author formulated and investigated a simplified 2-D model which could mimic the same dynamics of the 3-D model instead. However, the simplified model, which shortened the dynamics of wind and wave, might result in an unexpected problem. Reasonably, the optimal robust H_∞ controller was selected for stability warranted. The controller scheme is illustrated in Fig. 17, where α is the tower pitch angle compared with the vertical axis, β is blade pitch angle (BPA), ω_R is the rotor speed, and T_E is the generator output torque.

To verify the proposed solution, a simulation on both simplified 2-D model and FAST model under wind speed variations (12~25 m/s) was carried out. From the simulated test, the simplified model could be used as replacement the dynamic of the FAST model in general. Better speed performance was exhibited under the robust H_∞ controller; however, oscillations of both generator power and BPA change rate were increased in comparison with that of the baseline GSPI.

Improved from the previous work [86], Madsen et al. [87] investigated the quality of tension leg platform (TLP) under

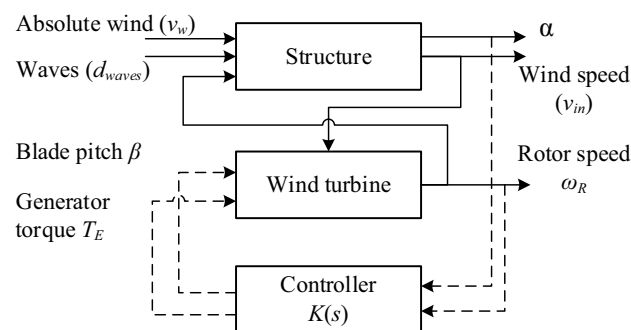


Fig. 17 Block diagram of the H_∞ controller. Reproduced with permission from [85]. Copyright 2014, IEEE

PI control not only for region 2 but also for region 3. The control strategy satisfied two requirements as (1) not excite the natural frequency of the system to avoid the resonance and (2) handle the "negative damping" behavior due to the relation between the CPC and structure dynamics at low-frequency mode. Therefore, the author considered two strategies corresponding to two working conditions as sketched in Fig. 18.

The first approach of the IPC on the TLP was reported in [88] by Namik. In this work, the author validated qualities of the 5-MW TLP under a disturbance accommodating controller (DAC) which was exploited to handle the wind disturbance. The DAC was exploited to mitigate the influence of perturbation in wind speed. In his contribution, three modified DAC algorithms were introduced and compared

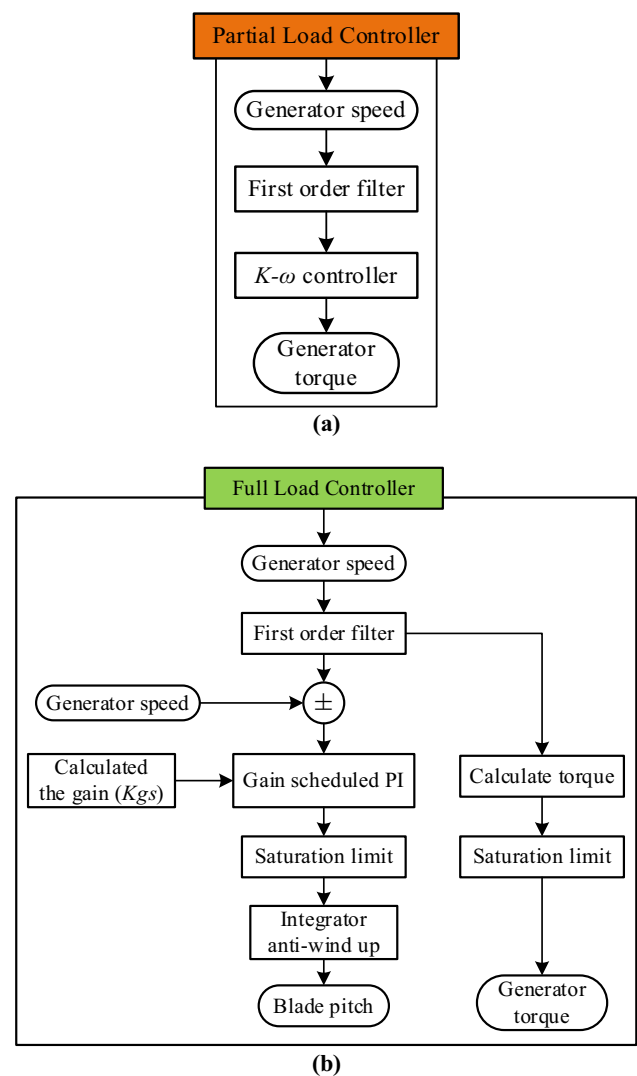


Fig. 18 Control strategy in: a region 2 with partial load and b region 3 with full load. Reproduced with permission from [87]. Copyright 2020, Elsevier

with the baseline GSPI controller proposed by Jonkman. By exploiting the DAC to reject the wind perturbation, the rotor speed regulation achieved an improvement of 73% and power performance achieved an improvement of 47% in comparison with that of baseline GSPI control; however, the blade fatigue loads were increased as discussed in previous works [81–86].

Inherited advantages from preliminary studies, in [89], the authors presented completely simulations of physical interactions and control strategies on both TLP and B-FOWT. Three controllers were selected for verifications. The first controller was the decentralized robust baseline control, the second one was SS-IPC, and the last one was the DAC to reject the influence of wind disturbance as shown in Fig. 19. In this figure, y is output, x is actual system state, u^{op} and x^{op} denote optimal control signal and optimal state, respectively; \hat{z} is an estimated disturbance waveform state vector. \bar{A}_{NR} , \bar{C}_{NR} , K_{NR} , E_{NR} are matrices for calculating estimated disturbance, and X_{NR} is an entity X transformed to the non-rotating frame of reference. $T_s(\psi)$, $T_c(\psi)$, and $T_o(\psi)$ are transformation matrices. More detail of control methodologies for further developing is presented in this material. The numerical simulation was run by using a FAST model and MATLAB/Simulink program under evaluative criteria such as fatigue loads, generator power and rotor speed error root mean square. The IEC-61400-3 standard for the offshore wind turbines was considered for varying wind-wave conditions. Criteria relating fatigue damage equivalent load, generator power and rotor speed error root mean square (RMS) and RMS of platform change rate RMS were provided for evaluations.

The simulated results indicated that the advanced controller could improve the system performance over the baseline control. Although the DAC extracted significant reductions of loads and platform movement on the TLP, this technique had less effect on the B-FOWT. A reason was this type of FOWT got strongly influenced by wave disturbances (3

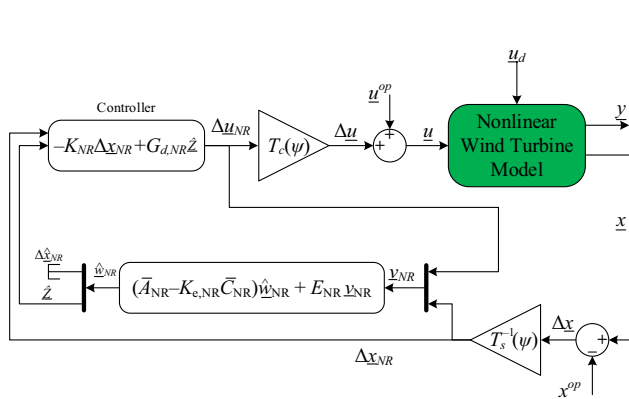


Fig. 19 Configuration of DAC algorithm. Reproduced with permission from [89]. Copyright 2011, Elsevier

times) rather than wind flows whereas the DAC was utilized for wind perturbation rejection. Even though, the fore-aft, side-side loads and platform behavior (rolling, pitching, and yawing) of the B-FOWT could be noticeably reduced when applying the IPC-SFC in comparison with that of the baseline. To the end, in comparison with the baseline GSPI, the SFC can achieve better performance in most indices of platform performances and fatigue loads. Among the state-space method, the IPC-SFC was suitable for the B-FOWT while better performance could be achieved by applying DAC on the TLP.

Took advantages of both CPC and IPC, the first configuration of CPC-IPC for the FOWT was reported by Zhang et al. in [90]. As aforementioned, the author aimed to employ the IPC-based trailing edge flap (TEF) technique to impair the fatigue DELs exerted on the blade and improve the generator speed by CPC. Meanwhile, the CPC accepted the generator speed, or power as similar, as the input and exported the collective blade pitch (CBP) θ as the control signal to manipulate the generator output, the IPC assigned a flap-wise root moment (FWRM) supposed to be measured of each blade and azimuth angle ϕ as inputs for designing the control algorithm. The Coleman transformation was utilized to transform coordinate between the FWRM coordinate to the fixed coordinate of the tower, vice versa, for calculating the TEF angle ϕ . These commanded parameters helped to reduce the influences of fatigue DELs induced from flap-wise and edge-wise vibration on the blade. The simulated results under different conditions shown that the FWRM could be noticeably attenuated. Then based on this construction, the author continuously developed his algorithm with speed and torque regulations to enhance the quality of the generator output as displayed in Fig. 20 [91]. In this research, the author applied the CPC-IPC on the 5-MW NREL TLP-FOWT and considered the system performance under Normal Turbulence Mode (NTM) and Normal Sea

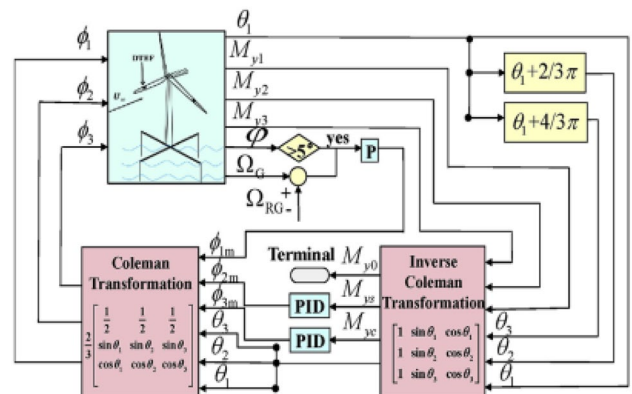


Fig. 20 Combination of CPC and IPC on the FOWT. Reproduced with permission from [91]. Copyright 2019, Elsevier

State (NSS) conditions. The comparative results indicated that all considered indices, especially the platform fore-aft motions in pitching and yawing, were improved in comparison with that of conventional controllers without considering TEF. Better performance obtained under flap control rather than the one without flap proved feasible potentials of the technique in realistic applications.

4.3 Control for FOWT with Spar Type (S-FOWT)

This type of FOWT is configured with a long vertical pillar in which the upper part is lighter, and the bottom is much heavier to exhibit a low center of gravity. This allows the structure to get more stable due to less getting affected from wave excitation. Different from the TLP or B-FOWT whose natural frequency is about 0.6 rad/s or 0.1 Hz, the S-FOWT has the lowest natural frequency (approximately 0.21 rad/s or 0.03 Hz), much lower than TLP and B-FOWT. The wave surge motion exerts up to 68% the platform pitch peak resonant frequency. Therefore, it is necessary to carefully consider these issues when designing control methodologies.

In [92], Larsen et al. investigated the dynamics of S-FOWT to design a suitable control strategy. The author firstly expressed the importance of the controller natural frequency over the system natural frequency. Here, three modes of low frequency were briefly introduced to avoid structure vibration. Additionally, the negative damping due to decreased thrust force as increasing value at above rated wind speed was figured out. Therefore, a controller that could adopt the system operation in three regions: variable optimal speed control for maximizing power at low wind speed (region 2), constant speed in near rated wind speed (region 2.5), and constant torque regulation to minimize powertrain loads at above rated wind speed (region 3) was designed. In region 2.5, the constant speed was set as the objective for the controller and the power linearly increased with respect to the wind speed. With the aim of achieving constant output generator torque in region 3, an active blade pitch angle (BPA) control is satisfied such that the measured BPA is regulated to a reference BPA. The BPA reference is calculated from the error of generator speed and its rated speed. Also this value is limited by upper and lower values that are determined based on wind speed and maximum value (90 degree). Same for the generator torque, the generator output torque is hold at the upper limitation (can be considered as rated value) in case of operation in region 3, and lower limitation in case of operation in region 2. The schematic diagram of this control was sketched in Fig. 21.

Based on the idea of power regulation and consideration of very high turbulent wind speed conditions, Ma et al. [93] investigated influence of the typhoon on the 5 MW OC3-Hywind Spar FOWT. To cope with this situation, the author constructed the cascaded control for power and speed

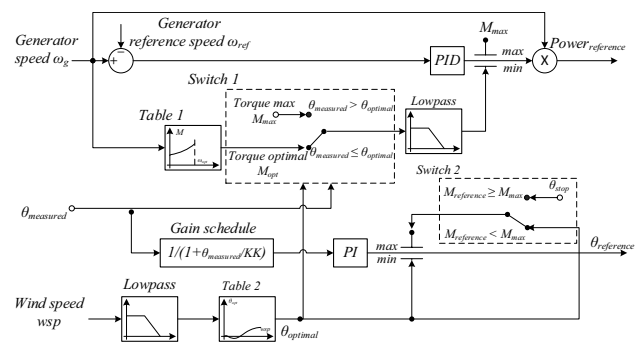


Fig. 21 Control strategy for S-FOWT in region 2 and 3. Reproduced with permission from [92]. Copyright 2007, IOP Science

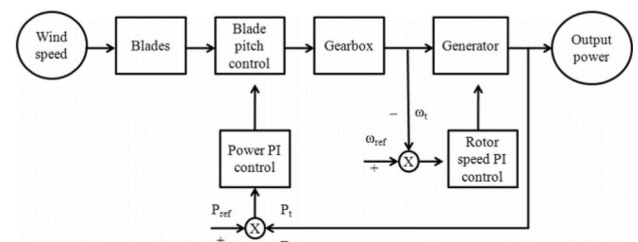


Fig. 22 CPC based on a cascaded control scheme. Reproduced with permission from [93]. Copyright 2017, Elsevier

manipulation as shown in Fig. 22. The GSPI was inherited for designing control algorithms. Additionally, to effectively design the control strategy and total system operation, effect of wave height was considered. For the typhoon environment, the author used a source from the typhoon “Damrey” by YOUNG05106L anemometer and 1 Hz frequency to export data for the wind profile. The value of wind speed was spread out in the interval of 11.4 to 25 m/s.

Fischer et al. [94] noticed the problem of non-minimum phase zeros (NMPZ). This problem appeared when a numerator of a transfer function between the generator speed and BPA returned a pair of roots lying on the half-right plane along with the natural frequency of the actuator when it reaches to a value near the system natural frequency (NF). Therefore, to cancel out this term and avoid the NMPZ, the nacelle velocity should be feedback to the controller. Moreover, the author introduced a switching function to shift the suitable controller for each region of operation as safety condition. The simulation indicated that the bandwidth of the closed-loop system could be increased by NMPZ compensator strategy and the stability of the system was enhanced with less overshoot.

From the ideal of feedback nacelle velocity for stabilization, Wakui et al. [95] considered the multi-variables feedback control and platform pitch angle to the output performance of the S-FOWT as shown in Fig. 23. Two feedback

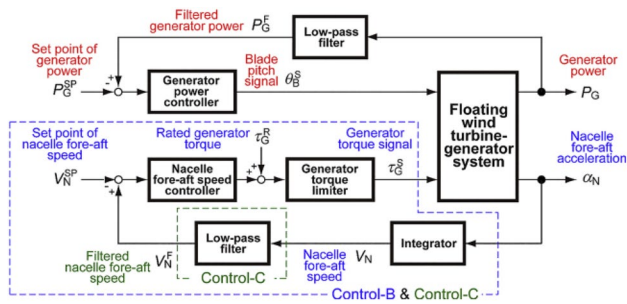


Fig. 23 Multi variable control algorithm. Reproduced with permission from [95]. Copyright 2017, Elsevier

loops including the baseline GSPI for a generator power control and a nacelle fore-aft speed control for generator torque regulation to stabilize the system were treated. Three controllers including baseline PI, MIMO control without a filter, and MIMO control with the filter (MIMO-F) were examined on the FAST model. Results indicated that the MIMO-F exhibited the least rotor speed, BPA, generator power fluctuation as well as reduced the platform pitch motion due to nacelle state feedback. However, higher fluctuated generator torque was extracted as the trade-off because the author considered the generator torque as a control input of the nacelle regulation.

Motivated from influences of different working regions (both regions 2 and 3), Oh et al. [96] investigated the system operation of the S-FOWT under different conditions of varying wind speed regions. Based on characteristics of high and low-frequency control, the author proposed a novel CPC which took advantages of both high control frequency pitch control (HPC) and low control frequency pitch control (LPC) as shown in Fig. 24 where Ω_g^{ref} and Ω_g denote the reference and measured generator speed, respectively. In addition, a tower acceleration feedback Control (TFC) and tower angular acceleration feedback control (TAFC) were introduced to increase the system damping. To verify the

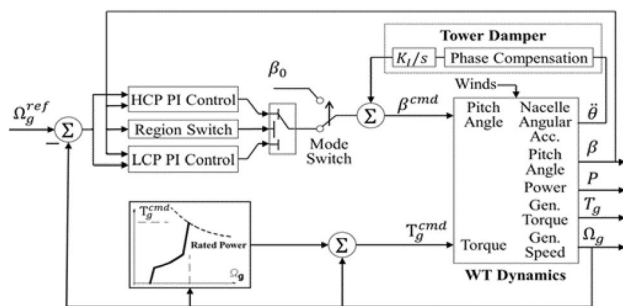


Fig. 24 The strategy of integrated HPC-LPC with tower damper configuration. Reproduced with permission from [96]. Copyright 2015, Springer

proposed algorithm, the simulation was implemented on the model of DNV-GL Bladed under the value of wind speed ranged from 13 to 25 m/s. Three different values of LPC frequency (0.1 rad/s, 0.15 rad/s, and 0.2 rad/s) and two different values of HPC (0.5 rad/s and 1 rad/s) were selected for investigating the platform dynamics. Regarding the simulation, when the wind speed was lower than 18 m/s, the LPC was considered with frequency of 0.2 rad/s; otherwise, the HPC was considered with the frequency of at least equal or higher 0.5 rad/s. The simulation confirmed that the blade and nacelle oscillation were significantly reduced by the tower damper, the bending moment of the tower was also reduced but less affected by the tower damper. The output power was slightly reduced as a result of increasing damper due to reducing the control frequency in pitch manipulated action.

Focused on deriving and investigating system dynamics, Zhu et al. [97] provided detailed descriptions about dynamics of the FOWT spar type. Then to consider the stable operation under high wind speed, the author constructed the control algorithm based on the conventional PI control with an anti-windup consideration. This consideration was to keep the action of the BPA from unexpected oscillations. Then the control algorithm was modified with added term K_s as illustrated in Fig. 25.

Same idea of using GS adaptive control, Yuan et al. [98] developed the methodology with the Disturbance Accommodating Control (DAC) to deal with disturbances induced from varying wind speed. Additionally, to handle other obstacles such as incompletely known system parameters, nonlinearities and uncertainties, the online parameter identification-based model reference adaptive control (MRAC) was employed along with the DAC along with DAC as shown in Fig. 26. The proposed methodology was compared with the baseline control under turbulent wind speed by simulation on 5-MW FAST model. The simulation results revealed that the MRAC-DAC and the DAC had quite the same response and could achieve better performances over the baseline controller. The results displayed that both DAC and MRAC-DAC could decrease the blade flapwise DELs up to 20% over GSPI and the MRAC-DAC could exhibit more stable performance such as speed and power regulation than that of DAC under the presence of uncertainties. The GSPI

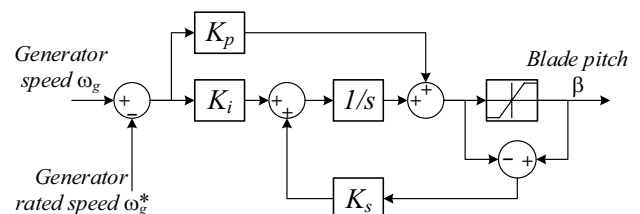


Fig. 25 Control algorithm with anti-wind up. Reproduced with permission from [97]. Copyright 2019, Elsevier

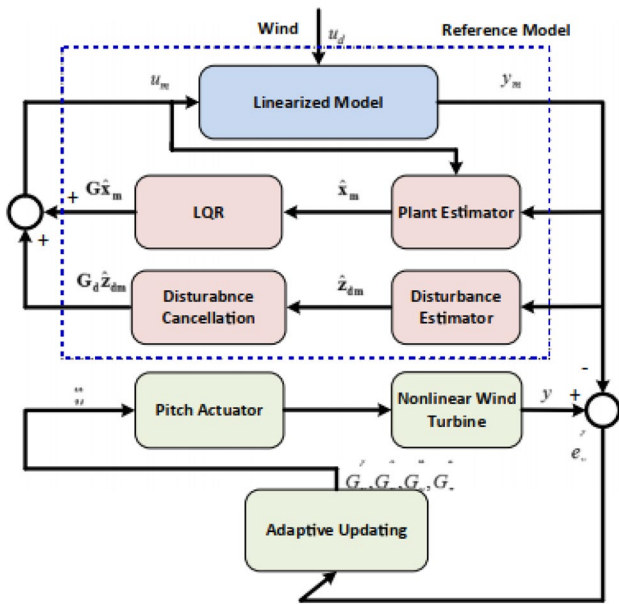


Fig. 26 Configuration of DAC-MRAC algorithm. Reprinted with permission from [98]. Copyright 2017, Elsevier

was only able to return the best performance in ideal cases when uncertainties were neglected.

The first IPC approach on the S-FOWT was reported in [99] by Namik et al. From the complete results acquisition on TLP and B-FOWT, the author investigated the S-FOWT response with the use of the DAC-based full state feedback control (FSFC) to observe and suppress the wind perturbation as displayed in Fig. 27. Besides, the degree-of-freedom (DOF) of surge motion was included. Excluding the surge-DOF out of the design when designing the SFC based on the linearized model could yield uncorrected frequency of the closed-loop system in regulating the blade pitch actuator. The detail about the influence of the certain number of DOF on the linearized SS was clearly discussed in this approach.

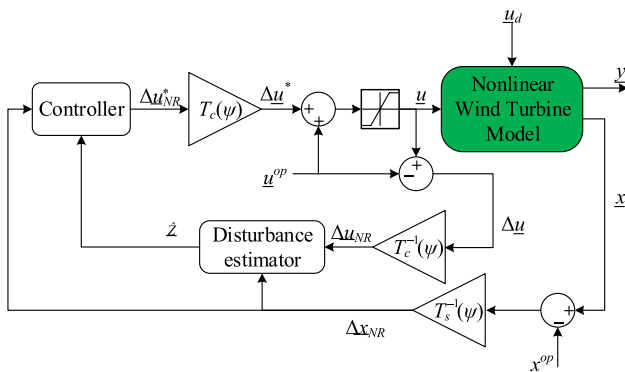


Fig. 27 Control strategy on the S-FOWT with DAC. Reproduced with permission from [99]. Copyright 2014, IEEE

The simulated results between the DAC and SFC over the baseline shown that the DAC could return better rotor speed performance while the SFC could result in more reduction of tower fatigue loads.

According to properties of the model predictive control (MPC) in predictability, Chaaban et al. [100] employed the MPC to cope with existing problems of fatigue load and platform pitching behavior arising from rotor speed control. The MPC block diagram is described in Fig. 28. In this configuration, the tower DEL, the platform pitching, and the generator power were assigned as inputs for configuring the MPC. To verify effectiveness of the proposed algorithm, numerical simulations was verified on the 5-MW NREL S-FOWT model under high wind speed of 18 m/s. The simulation results indicated that the use of MPC could exhibit better performance. Moreover, the MPC was capable of dealing with conflicts between speed and torque regulations in usual controllers and issue relating actuator saturation and its change rate.

In [101], Raach et al. employed the IPC-based nonlinear MPC (NMPC) to mitigate the blade fatigue loads. The idea of using the NMPC relied on its advantages of including all considerable constraints and predicting future behaviors to optimize input command. The effectiveness of the NMPC was verified by comparative simulations with baseline control (BC) and extended baseline IPC (BIPC). The simulations was implemented under the scenario of turbulent wind speed. The control objective were to reduce the blade pitch fatigue loads and regulate the rotor speed at a constant rated value. The generator torque was fixed at constant value under the BC and BIPC. Totally, the steady output generator power was indirectly obtained via speed regulation. The simulation was initialized at an operation point to avoid transient responses. From the simulated results, the NMPC returned the best qualities in most evaluated indices and significant reduction of the fatigue loads.

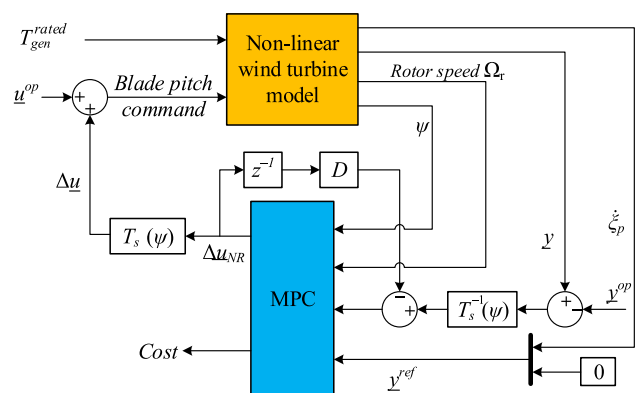


Fig. 28 Control algorithm based on MPC technique [100]

In the trend of studying and developing more effective algorithms for the FOWT, Yang et al. [102] proposed a novel method for IPC which employed the DAC integrated with MPC to reduce loads induced from wind-wave disturbances and to regulate the blade pitch actuation to follow the desired trajectory determined from an undisturbed reference baseline control 5-MW S-FOWT model formulated by Jonkman. For effective integration, the FLC was designed to associate the DAC and MPC and update gains as shown in Fig. 29. From the comparative simulation between CPC and IPC on the FAST model, the proposed control could export better robustness under turbulent wind and wave interactions rather than conventional CPC in most evaluated indices.

Taking advantages of state feedback control (SFC), Sarkar et al. [103] proposed the idea of integrating a linear-quadratic (LQ) control with an integrated controller (LQ-I) to improve the generator output and spar-platform dynamics as shown in Fig. 30. The LQ control could help to improve the platform fore-aft motions (tower fore-aft and platform pitching movement) and reduce the 1P fluctuation on the blade. The rotor speed regulation was utilized by the integral controller. To prove the reliability of the proposed algorithm (LQ-I: Linear-quadratic with Integral control) in comparison with that of baseline and conventional IPC, numerical simulations on the 5 MW OC3 Hywind S-FOWT under steady wind without waves and different wind-waves interaction were implemented. The simulated results certified that the proposed LQ-I returned a better fatigue DEL reduction than SFC and DAC in [93]. Also, the output power regulation was better than DAC and SFC method even when the DAC and SFC employed constant power control, not from IPC, to achieve the steady output power. Moreover, another

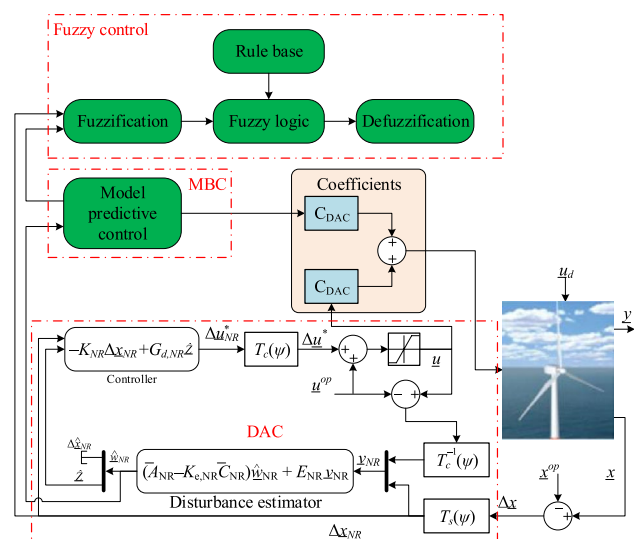


Fig. 29 Schematic diagram of the Fuzzy-DAC-MRAC algorithm. Reproduced with permission from [102]. Copyright 2014, Hindawi

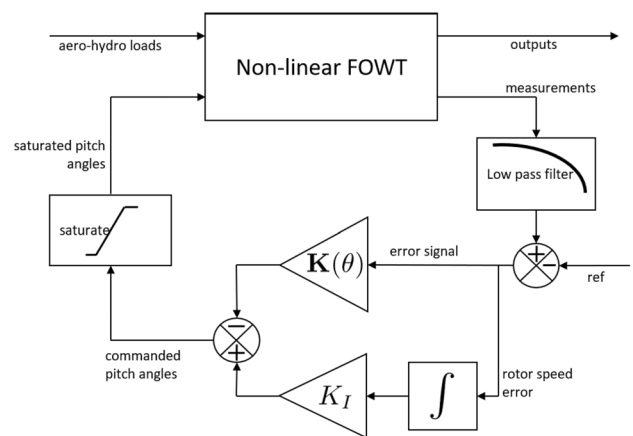


Fig. 30 Proposed linear quadratic integrated with Integral (LQ-I) control. Reproduced with permission from [103]. Copyright 2020, IEEE

comparison between the proposed LQ-I and a Nonlinear MPC in [101] also exported that better performance could be obtained from the proposed algorithm.

As comparison with the previous works, the integration of the SFC and one more component (like integral block in [103] to compensate the accumulated error) can exhibit the best performance in which most remained problems are tackled.

4.4 Control for FOWT with Semi-submersible Type (SS-FOWT)

A semi-submersible substructure is a semi-water plane stabilized floating buoy. The floating buoy is configured in triangular frame as shown in Fig. 31.

Despite being initialized long time ago, most works on this structure, up to now, were mainly focused on analyzing

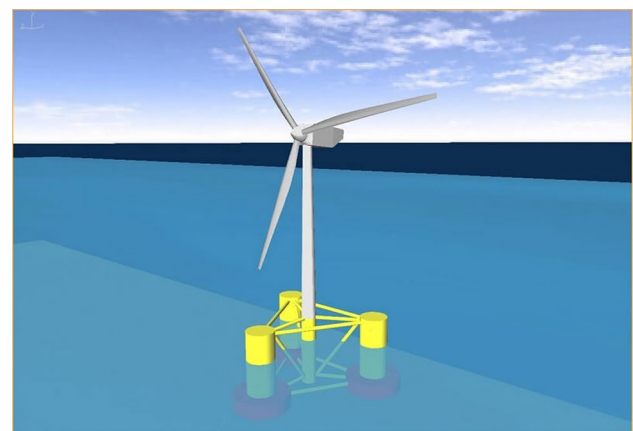


Fig. 31 Configuration of semi-submersible FOWT

and optimizing its structure and completing its coupled dynamics. Not many researches on this structure which considered control strategies were reported.

Yu et al. [104] first experimented a SS-FOWT test bench with CPC based GS to investigate effects of control algorithm to the system performance. The control structure was based on the baseline GSPI. The experiment was setup on the 1:60 scaled DTU 10 MW test bench model under influences of irregular wave and regular wave.

Taking consideration of the global performance, Goupee et al. examined the effects of the CPC and a power manipulation to the system dynamics under different control strategies [105]. The four considerable controllers including variable speed (VS) control, constant speed control CS25, CS100 and the baseline FF (fixed rotor speed fixed pitch angle) algorithm were selected and applied on the DeepCwind-OC5 semi-submersible FOWT in MARIN’s offshore basin laboratory. From the comparative results, the baseline FF manipulated the largest generator torque variation. The VS exported the best performance with the least fluctuated torque; however, the speed regulation under the VS control got the largest fluctuation whereas the other three controllers showed the mostly constant speed performance. Between the C25 and C100, the C100 with larger gains could ensure a significant reduction of platform surge behavior but extract larger tower pitch motion conversely. In the contrary, the C25 could gain a larger interval of pitch actuation due to slow response in blade pitch mechanism. In general, the VS returned the best global performance, then the C100, and the C25.

Studied about the SS-FOWT, Kim et al. [106] realized influences of designing CPC parameters on performances of the 5-MW OC4 SS-FOWT and 3-MW KRISO multi-unit FOWT (MUFOWT) with the use of the FAST-CHARM3D. To complete the examination, the author applied a controller as shown in Fig. 32 on the two models and investigated the effects of selecting CPC natural frequency and CPC damping ratio (DR) to output under different scenarios.

From the comparative simulation, the author stated that the best generator power action could be established while the value of the CPC damping ratio was 0.6–0.7. The design of CPC natural frequency was important to achieve good output performance. Better performance could be established with a suitable value of CPCNF against the platform pitch NF, and poor performance was exhibited with unsuitable value, conversely.

In [107], Lemmer et al. clarified not only a trade-off between the speed regulation and structure global performance but also discussed an issue of the so-called inverse-response. This issue occurred when the zeros of the transfer function between the blade rotor speed and pitch actuator were on the right-half plane. This indicated that the frequency of zeros matched with fore-aft modes

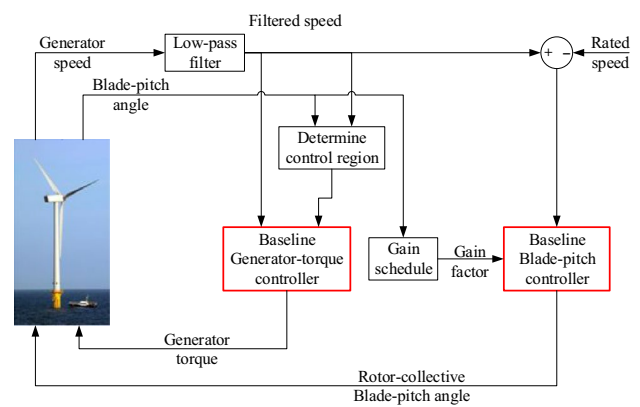


Fig. 32 A baseline GSPI applied on the SS-FOWT. Reproduced with permission from [106]. Copyright 2018, Techno-Press

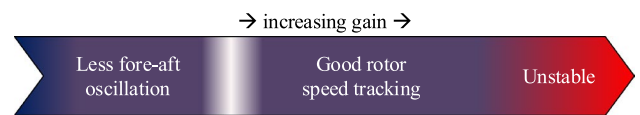


Fig. 33 Indicated tradeoff when adjusting control gains. Reproduced with permission from [107]. Copyright 2019, John Wiley & Sons, Ltd

natural frequency. Therefore, the author proposed a robust in which the control gains were carefully considered to handle the trade-off between generator speed and system response as shown in Fig. 33.

Two control configurations were presented as single-input-single-output (SISO) and multi-input-multi-output (MIMO) controllers. For multiple variable systems, multi-SISO based on a decentralized method was designed. The MIMO strategy was designed based on several previous approaches. Hence, the "tailored coupled control-oriented model" was proposed to obtain the GSPI based SISO control scheme. Instead of using a standalone generator speed parameter, the azimuth angle was added into the controller design as described in Eq. (8).

$$\Delta\beta = \frac{k_p(\beta)}{i_{gear}} \Delta\omega + \frac{k_p(\beta)}{i_{gear}T_i} \Delta\varphi \tag{8}$$

where $k_p(\theta)$ and $k_p(\theta)/T_i$ denote the proportional and integral gains, $\Delta\varphi$ is the azimuth angle error, $\Delta\omega$ is the generator speed error effort, and i_{gear} is the transmission ratio, β is the blade pitch angle.

Numerical results indicated that the robust gains for GSPI with the so-called tailored coupled control-oriented could tackle existing problems. Besides, the comparison between the proposed method-based standard SISO framework to the conventional baseline and MIMO LQR was carried out to

highlight its advantages in achieving more robust and tackling all FAST dynamics uncertainties.

Considered a wind farm, Han et al. [108] aimed to optimize the output power and reduce the wake effect by considering not only blade pitch angle, but also platform orientation and position. The cascaded control was suggested and applied to one sampled floated as displayed in Fig. 34. First, the power requested, and position target were predetermined based on the local demand and information of wind-waves interaction. Then the current position was controlled to a target (P_{tar}) throughout position control with an orientation variable γ , and actual power was manipulated to the power requested by power regulation. The commanded pitch angle was a production of the position control and stabilizing control. The simulation on the OC4-DeepCwind semi-submersible FOWT under the presence of disturbance was given with comparisons between a linear-quadratic integrator (LQI) controller based on state feedback, PID control and open-loop response. The simulated results confirmed that the proposed LQI could guarantee the best system stability against the influence of the environment (wind and wave disturbance).

5 Conclusions and Future Work

Though there was a rapid growth of wind energy, especially at onshore, during last decades, many countries are facing the limitation of wind turbine expansion because of the geological restriction and social objections mainly caused from the noise. As an alternative choice and the idea in the view of exploration of vast ocean with unlimited wind resource, the offshore wind turbines were getting many attentions and led to continuous growth with innovative technology. As the size and capacity of wind turbines are getting bigger mostly for raising economic scale related to the reduction of LCOE, the advanced control technologies have been attracting more attention for the performance improvement and the efficient integration of wind turbine system. Moreover, for

floating offshore wind turbine (FOWT), the adequate selection of control technologies becomes more important not only because of the high reliable energy production, but also because of the motion stability.

Generally, there are two main control strategies: (1) collective blade pitch control (CPC), and (2) individual blade pitch control (IPC) in designing of control schemes for the FOWT. According to characteristics of each type of control, the CPC can achieve good performance in rotor or generator speed, and power regulation, but facing with other problems of torque variation and platform qualification. On the contrary, the IPC can deal with the torque variation due to its control strategy, and improve platform qualification (rolling and yawing motions, loads). However, this method cannot ensure the speed regulation. Besides, fluctuations (induced from flap-wise and edge-wise vibrations) cause more load on blades to increase. Recently, a combination of CPC in achieving good speed and power regulation and IPC for canceling blade fluctuations is suggested. However, this technique is only investigated on the TLP type. It means there are many opportunities for researchers to further study on other type of the FOWT. Besides, various control methodologies as discussed above could be integrated to enhance system performance. From the view of control methodologies, the baseline GSPI control is the most suitable for all type of the FOWT. However, this method remains the trade-off between the generator output power and torque, and thus, affecting other relevant performances such as fore-aft, side-side motions, fatigue loads, and oscillations. Therefore, the state feedback control (SFC) strategies known as optimal control have been developed to cover all existing problems in system level. Despite earning optimal controllers, designing of the SFC is much more difficult since it requires a well-known knowledge of system dynamics. Besides, different methodologies result in different qualifications when applying on specific foundations. For instance, the use of DAC can achieve better performance for the TLP type, but not for the barge type due to its characteristic of water-plane foundation. Using the conventional SFC is more suitable for this floater. Therefore, one should carefully consider foundation characteristics for suitable design of control in term of system level.

This review especially explores the recent control techniques for floating offshore wind turbine with different substructure types such as barge type, tension-leg platform (TLP) type, spar type, and semi-submersible type. Advantages and disadvantages between each algorithm were discussed and comparisons according to the application of the same algorithms to different floater type were also handled. Table 4 summarizes the control algorithms reviewed for this paper.

The improvements of control technologies will definitely lead to the cost reduction related to O&M (operations and

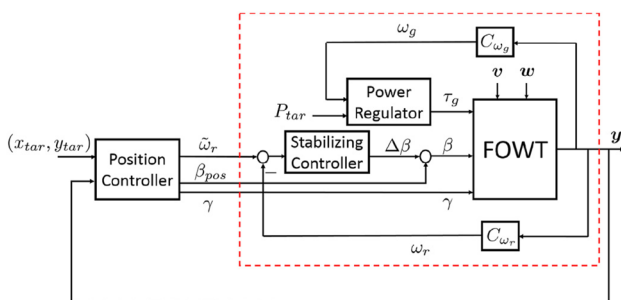


Fig. 34 Multi-objective control algorithm for SS-FOWT. Reprinted with permission from [108]. Copyright 2020, Elsevier

Table 4 Control algorithms for FOWTs

Type	Algorithms	
	CPC	IPC
Barge	GSPI SFC LQR LPV-GS	SFC
TLP	GSPI H ∞	SFC DAC PID-based CPC-IPC
Spar	GSPI MIMO-based PI HPC-LPC-TFC DAC	SFC MRAC-DAC MPC Fuzzy-MRAC-DAC LQ-I
Semi-submersible	GSPI MIMO-based PI MIMO-based SFC	NA (Not Available)

maintenance) while keeping the performance of FOWT at its best, which will make wind turbines more competitive and will increase AEP (annual energy production) in the level of a large wind farm operation.

Acknowledgement This work was supported by Brain Pool Program through the National Research Foundation of Korea (NRF) funded by the Ministry of Science and ICT (2019H1D3A2A02102093) and by Basic Science Program through the National Research Foundation of Korea (NRF) funded by the MSIT(2020R1A2B5B03001480).

References

- Musial, W. et al. (2018). U.S. Department of Energy. 2018 Offshore Wind Technologies Market Report
- Castro-Santos, L., Filgueira, A., Alvarez, J., & Carral, L. (2018). Influence of size on the economic feasibility of floating offshore wind farms. *Sustainability*, 10, 4484. <https://doi.org/10.3390/su10124484>.
- Wiser, R., Jenni, K., Seel, J., Baker, E., Hand, M., Lantz, E., et al. (2016). Expert elicitation survey on future wind energy costs. *Nature Energy*, 1, 16135. <https://doi.org/10.1038/nenergy.2016.135>.
- Wehrmann, B. (2018). Offshore wind power in Germany: Power production at sea re-emerges as Energiewende cornerstone, Clean Energy Wire, <https://www.cleanenergywire.org/dossiers/offshore-wind-power-germany>, May 4, 2018.
- Betz, A. (1926). Windenergie und Ihre Ausnutzung durch Windmullen. Vandenhoek and Ruprecht Gottingen
- Lawrence Berkeley National Laboratory. (2019). “R&D Pathways for supersized wind turbine blades”, DNVGL, Document No.: 10080081-HOU-R-01, March 2019.
- Ha, K., Bätge, M., Melcher, D., & Czichon, S. (2020). Development and feasibility study of segment blade test methodology. *Wind Energy Science*, 5(2), 591–599. <https://doi.org/10.5194/wes-5-591-2020>.
- Bladena. (2019). “Wind turbine blades handbook”, Kirt & Thomson, ISBN 978-87-971709-0-8.
- Bronsted, P., & Nijssen, R. P. (2013). *Advances in wind turbine blade design and materials*. UK: Woodhead Publishing Series in Energy.
- Zhu, W. J., Shen, W. Z., & Sørensen, J. N. (2014). Integrated airfoil and blade design method for large wind turbines. *Renewable Energy*, 70, 172–183. <https://doi.org/10.1016/j.renene.2014.02.057>.
- Bertagnolio, F., Sørensen, N.N., Johansen, J., & Fuglsang, P. (2001). “Wind turbine airfoil catalogue”, Denmark. Forskningscenter Risoe, Risoe-R. No. 1280(EN).
- Grasso, F. (2012). Development of thick airfoils for wind turbines. Presented at 50th AIAA Aerospace Sciences Meeting. AIAA2012-0236.
- WindEurope. (2019). Offshore wind in Europe: Key trends and statistics 2018. <https://windeurope.org/wp-content/uploads/files/about-wind/statistics/WindEurope-Annual-Offshore-Statistics-2018.pdf>.
- Global Wind Energy Council. (2020). Global wind report 2019. <https://gwec.net/global-wind-report-2019/>.
- Konstantinidis, E. I., & Botsaris, P. N. (2016). Wind turbines: Current status, obstacles, trends, and technologies. *IOP Conference Series: Materials Science and Engineering*. <https://doi.org/10.1088/1757-899X/161/1/012079>.
- Wehrmann, B. (2020). German offshore wind power—Output, business, and perspectives, Clean Energy Wire, <https://www.cleanenergywire.org/factsheets/german-offshore-wind-power-output-business-and-perspectives>. April 17, 2020.
- Sirnivas, S., Musial, W., Bailey, B., & Filippelli, M. (2014). Assessment of offshore wind system design, safety, and operation standards. NREL/TP-5000-60573, National Renewable Energy Laboratory.
- Teh, N. (2019). Japan & South Korea Floating Offshore Wind 2019, Innovate UK Global Expert Mission.
- Statoil, Hywind Scotland Pilot Park: Environmental Statement, Document number: A-100142-S35-EIAS-001, April 2015.
- IRENA. (2016). *Floating foundations: A game changer for offshore wind power*. Abu Dhabi: International Renewable Energy Agency.
- IRENA. (2019). *Future of wind: Deployment, investment, technology, grid integration and socio-economic aspects (A Global Energy Transformation paper)*. Abu Dhabi: International Renewable Energy Agency.
- Nguyen, H., & Naidu, D. (2013). Evolution of Wind Turbine Control Systems. In *Encyclopedia of control systems, robotics, and automation* (pp. 1–50). Oxford, UK: EOLSS Publishers.
- Jonkman, J. M. (2009). Dynamics of offshore floating wind turbines—model development and verification. *Wind Energy*, 12, 5. <https://doi.org/10.1002/we.347>.
- Erdozain, J.O., Elorza, I., Calleja, C., Jugo, J., & Pujana-Arrese, A. (2017). *Advanced control for floating offshore wind turbine*. Ikerlan: The III Marine Energy Week.
- Manwell, J. F., et al. (2002). *Wind energy explained: Theory, design and applications*. USA: Wiley. **Chapter 3**.
- Burton, T., Jenkins, N., Sharpe, D., & Bossanyi, E. (2011). *Wind energy handbook* (2nd ed.). USA: Wiley. <https://doi.org/10.1002/9781119992714>.
- Hau, E., & Turbines, W. (2013). *Fundamentals, technologies, application, economics*. Berlin: Springer.
- Mahmoud, M.S., & Xia, Y. (2012). Some industrial systems. In: *Applied control systems design*, chapter 2, London: Springer.
- Damiani, R., et al. (2016). A comparison study of offshore wind support structures with monopiles and jackets for US waters. *Journal of Physics: Conference Series*. <https://doi.org/10.1088/1742-6596/753/9/092003092003>.
- Van-der-Valk, P. (2014). Coupled simulations of wind turbines and offshore support structures: Strategies based on the

- dynamic substructuring paradigm. Doctoral thesis. <https://doi.org/10.4233/uuid:ac619319-9eae-443d-8b94-d0246f80ffdb>. <https://repository.tudelft.nl/islandora/object/uuid%3Aac619319-9eae-443d-8b94-d0246f80ffdb>.
31. DNVGL, DNVGL-ST-0119: Floating wind turbine structures, DNV GL AS, July 2018.
 32. Sarmiento, J., & Guanache, R. (2018). Day 1: Introduction to Off-shore Wind Fixed Structures. Short course. In *Hydrodynamics of fixed and floating Offshore Wind Turbine Foundations*. MaRI-NET2, Short-Course 3, 20–22 November 2018. The Netherlands: Wageningen.
 33. Faltinsen, O. M. (1990). *Sea loads on ships and offshore structures*. Cambridge: Cambridge University Press.
 34. Jonkman, J. (2007). Dynamics modeling and loads analysis of an offshore floating wind turbine. NREL/TP-500-41958. Golden, CO: National Renewable Energy Laboratory, November 2007.
 35. Yu, L., Bhattacharya, S., Li, L., & Guo, Z. (2014). Dynamic characteristics of offshore wind turbines on different types of foundations. *Electronic Journal of Geotechnical Engineering*, 19, 2917–2936.
 36. Tempel, J., Diepeveen, N., de Vries, W., & Salzmann, D. (2011). Offshore environmental loads and wind turbine design: Impact of wind, wave, currents, and ice (pp. 463–478). <https://doi.org/10.1533/9780857090638.4.463>.
 37. Bai, Y., & Jin, W.-L. (2016). Loads and dynamic response for offshore structures. <https://linkinghub.elsevier.com/retrieve/pii/B9780080999975000071>.
 38. Leimeister, M., Kolios, A., & Collu, M. (2018). Critical review of floating support structures for offshore wind farm deployment. *IOP Conference Series*, 1104(2018), 012007. <https://doi.org/10.1088/1742-6596/1104/1/012007>.
 39. Bianchi, F. D., de Battista, H., & Mantz, R. J. (2007). *Wind turbine control systems: Principles, modelling and gain scheduling design*. London: Springer-Verlag.
 40. Lucy, Y. P., & Kathryn, E. J. (2011). Control of wind turbines: Approaches, challenges, and recent developments. *IEEE Control Systems Magazine*. <https://doi.org/10.1109/MCS.2010.939962>.
 41. Novaes Menezes, E. J., Araújo, A. M., & Bouchonneau da Silva, N. S. (2018). A review on wind turbine control and its associated methods. *Journal of Cleaner Production*, 174, 945–953. <https://doi.org/10.1016/j.jclepro.2017.10.297>.
 42. Kumar, D., & Chatterjee, K. (2016). A review of conventional and advanced MPPT algorithms for wind energy systems. *Renewable and Sustainable Energy Reviews*, 55, 957–970. <https://doi.org/10.1016/j.rser.2015.11.013>.
 43. Chatterjee, S., & Chatterjee, S. (2018). Review on the techno-commercial aspects of wind energy conversion system. *IET Renewable Power Generation*, 12(14), 1581–1608. <https://doi.org/10.1049/iet-rpg.2018.5197>.
 44. Tiwari, R., & Babu, N. R. (2016). Recent developments of control strategies for wind energy conversion system. *Renewable and Sustainable Energy Reviews*, 66, 268–285. <https://doi.org/10.1016/j.rser.2016.08.005>.
 45. Do, H. T., Dang, T. D., Truong, H. V. A., & Ahn, K. K. (2018). Maximum power point tracking and output power control on pressure coupling wind energy conversion system. *IEEE Transactions on Industrial Electronics*, 65(2), 1316–1324. <https://doi.org/10.1109/tie.2017.2733424>.
 46. Nguyen, M. T., Dang, T. D., & Ahn, K. K. (2019). Application of electro-hydraulic actuator system to control continuously variable transmission in wind energy converter. *Energies*, 12(13), 2499. <https://doi.org/10.3390/en12132499>.
 47. Luo, X., & Niu, S. (2017). A novel contra-rotating power split transmission system for wind power generation and its dual mppt control strategy. *IEEE Transactions on Power Electronics*, 32(9), 6924–6935. <https://doi.org/10.1109/tpe.2016.2629021>.
 48. Yin, X.-X., Lin, Y.-G., Li, W., & Gu, H.-G. (2016). Hydro-viscous transmission based maximum power extraction control for continuously variable speed wind turbine with enhanced efficiency. *Renewable Energy*, 87, 646–655. <https://doi.org/10.1016/j.renene.2015.10.032>.
 49. Wei, L., Liu, Z., Zhao, Y., Wang, G., & Tao, Y. (2018). Modeling and control of a 600 kW closed hydraulic wind turbine with an energy storage system. *Applied Sciences*, 8(8), 1314. <https://doi.org/10.3390/app8081314>.
 50. Petković, D., Čojbašić, Ž., Nikolić, V., Shamshirband, S., Mat Kiah, M. L., Anuar, N. B., et al. (2014). Adaptive neuro-fuzzy maximal power extraction of wind turbine with continuously variable transmission. *Energy*, 64, 868–874. <https://doi.org/10.1016/j.energy.2013.10.094>.
 51. Yin, X.-X., Lin, Y.-G., & Li, W. (2015). Operating modes and control strategy for megawatt-scale hydro-viscous transmission-based continuously variable speed wind turbines. *IEEE Transactions on Sustainable Energy*, 6(4), 1553–1564. <https://doi.org/10.1109/tste.2015.2455872>.
 52. Kim, K., Kim, H.-G., Kim, C.-J., Paek, I., Bottasso, C. L., & Campagnolo, F. (2018). Design and validation of demanded power point tracking control algorithm of wind turbine. *International Journal of Precision Engineering and Manufacturing-Green Technology*, 5(3), 387–400. <https://doi.org/10.1007/s40684-018-0041-6>.
 53. Kim, K., Kim, H., Paek, I., Kim, H.-G., & Son, J. (2019). Field validation of demanded power point tracking control algorithm for medium-capacity wind turbine. *International Journal of Precision Engineering and Manufacturing-Green Technology*, 6(5), 875–881. <https://doi.org/10.1007/s40684-019-00107-3>.
 54. Yin, X., Tong, X., Zhao, X., & Karcianas, A. (2020). Maximum power generation control of a hybrid wind turbine transmission system based on H ∞ loop-shaping approach. *IEEE Transactions on Sustainable Energy*, 11(2), 561–570. <https://doi.org/10.1109/tste.2019.2897549>.
 55. Yin, X.-X., Lin, Y.-G., Li, W., Gu, Y.-J., Liu, H.-W., & Lei, P.-F. (2015). A novel fuzzy integral sliding mode current control strategy for maximizing wind power extraction and eliminating voltage harmonics. *Energy*, 85, 677–686. <https://doi.org/10.1016/j.energy.2015.04.005>.
 56. Yin, X.-X., Lin, Y.-G., Li, W., Liu, H.-W., & Gu, Y.-J. (2014). Output power control for hydro-viscous transmission based continuously variable speed wind turbine. *Renewable Energy*, 72, 395–405. <https://doi.org/10.1016/j.renene.2014.07.010>.
 57. Yin, X., Jiang, Z., & Pan, L. (2020). Recurrent neural network based adaptive integral sliding mode power maximization control for wind power systems. *Renewable Energy*, 145, 1149–1157. <https://doi.org/10.1016/j.renene.2018.12.098>.
 58. Navarrete, E. C., Trejo Perea, M., Jauregui Correa, J. C., Carrillo Serrano, R. V., & Moreno, G. J. R. (2019). Expert control systems implemented in a pitch control of wind turbine: A review. *IEEE Access*, 7, 13241–13259. <https://doi.org/10.1109/access.2019.2892728>.
 59. Pelin, R. I., Bărsănescu, P. D., & Țița, I. (2018). Hydraulic systems used for pitch control of wind turbines: a literature overview. *IOP Conference Series: Materials Science and Engineering*, 444(4), 042013.
 60. Li, Y., Liu, S., Wang, J., Zhang, H., & Lu, Z. (2009). Design of control system for wind turbine electric pitch. 2009 International Conference on Measuring Technology and Mechatronics Automation, Zhangjiajie, Hunan, pp. 50–53. <https://doi.org/10.1109/ICMTMA.2009.29>.
 61. Song, D., Yang, J., Su, M., Liu, A., Cai, Z., Liu, Y., et al. (2017). A novel wind speed estimator-integrated pitch control method for wind turbines with global-power regulation. *Energy*, 138, 816–830. <https://doi.org/10.1016/j.energy.2017.07.033>.

62. Yin, X.-X., Lin, Y.-G., Li, W., Gu, Y.-J., Wang, X.-J., & Lei, P.-F. (2015). Design, modeling and implementation of a novel pitch angle control system for wind turbine. *Renewable Energy*, *81*, 599–608. <https://doi.org/10.1016/j.renene.2015.03.042>.
63. Zhang, Y., Cheng, M., & Chen, Z. (2013). Proportional resonant individual pitch control for mitigation of wind turbines loads. *IET Renewable Power Generation*, *7*(3), 191–200. <https://doi.org/10.1049/iet-rpg.2012.0282>.
64. Bossanyi, E. A. (2003). Individual blade pitch control for load reduction. *Wind Energy*, *6*(2), 119–128. <https://doi.org/10.1002/we.76>.
65. Yuan, Y., Chen, X., & Tang, J. (2020). Multivariable robust blade pitch control design to reject periodic loads on wind turbines. *Renewable Energy*, *146*, 329–341. <https://doi.org/10.1016/j.renene.2019.06.136>.
66. Liew, J., Lio, W. H., Urbán, A. M., Holierhoek, J., & Kim, T. (2020). Active tip deflection control for wind turbines. *Renewable Energy*, *149*, 445–454. <https://doi.org/10.1016/j.renene.2019.12.036>.
67. Venkaiah, P., & Sarkar, B. K. (2020). Hydraulically actuated horizontal axis wind turbine pitch control by model free adaptive controller. *Renewable Energy*, *147*, 55–68. <https://doi.org/10.1016/j.renene.2019.08.127>.
68. Wang, C.-S., & Chiang, M.-H. (2016). A novel pitch control system of a large wind turbine using two-degree-of-freedom motion control with feedback linearization control. *Energies*, *9*(10), 791. <https://doi.org/10.3390/en9100791>.
69. Chiang, M.-H. (2011). A novel pitch control system for a wind turbine driven by a variable-speed pump-controlled hydraulic servo system. *Mechatronics*, *21*(4), 753–761. <https://doi.org/10.1016/j.mechatronics.2011.01.003>.
70. Yin, X. X., Lin, Y. G., Li, W., Liu, H. W., & Gu, Y. J. (2015). Adaptive sliding mode back-stepping pitch angle control of a variable-displacement pump controlled pitch system for wind turbines. *ISA Transactions*, *58*, 629–634. <https://doi.org/10.1016/j.isatra.2015.07.006>.
71. Yin, X.-X., Lin, Y.-G., Li, W., & Gu, Y.-J. (2014). Integrated pitch control for wind turbine based on a novel pitch control system. *Journal of Renewable and Sustainable Energy*, *6*(4), 043106. <https://doi.org/10.1063/1.4890566>.
72. Yin, X.-X., Lin, Y.-G., Li, W., Gu, Y.-J., Lei, P.-F., & Liu, H.-W. (2015). Adaptive back-stepping pitch angle control for wind turbine based on a new electro-hydraulic pitch system. *International Journal of Control*, *88*(11), 2316–2326. <https://doi.org/10.1080/00207179.2015.1041554>.
73. Yin, X., Zhang, W., Jiang, Z., & Pan, L. (2019). Adaptive robust integral sliding mode pitch angle control of an electro-hydraulic servo pitch system for wind turbine. *Mechanical Systems and Signal Processing*, *133*. <https://doi.org/10.1016/j.ymssp.2018.09.026>.
74. Colombo, L., Corradini, M. L., Ippoliti, G., & Orlando, G. (2020). Pitch angle control of a wind turbine operating above the rated wind speed: A sliding mode control approach. *ISA Transactions*, *96*, 95–102. <https://doi.org/10.1016/j.isatra.2019.07.002>.
75. Yin, X.-X., Lin, Y.-G., Li, W., Liu, H.-W., & Gu, Y.-J. (2015). Fuzzy-logic sliding-mode control strategy for extracting maximum wind power. *IEEE Transactions on Energy Conversion*, *30*(4), 1267–1278. <https://doi.org/10.1109/tec.2015.2422211>.
76. Han, B., Yang, F., Xiang, Z., & Zhou, L. (2016). Individual pitch controller based on fuzzy logic control for wind turbine load mitigation. *IET Renewable Power Generation*, *10*(5), 687–693. <https://doi.org/10.1049/iet-rpg.2015.0320>.
77. Yin, X.-X., Lin, Y.-G., & Li, W. (2016). Predictive pitch control of an electro-hydraulic digital pitch system for wind turbines based on the extreme learning machine. *Transactions of the Institute of Measurement and Control*, *38*(11), 1392–1400. <https://doi.org/10.1177/0142331215589610>.
78. Lackner, M. A., & van Kuik, G. (2010). A comparison of smart rotor control approaches using trailing edge flaps and individual pitch control. *Wind Energy*, *13*(2–3), 117–134. <https://doi.org/10.1002/we.353>.
79. <https://questfwe.com/documentation-center/moorings/>.
80. Bagherieh, O., & Nagamune, R. (2015). Gain-scheduling control of a floating offshore wind turbine above rated wind speed. *Control Theory and Technology*, *13*(2), 160–172. <https://doi.org/10.1007/s11768-015-4152-0>.
81. Namik, H., & Stol, K. (2009). Control methods for reducing platform pitching motion of floating wind turbines. 2009 European offshore wind, Stockholm.
82. Namik, H., & Stol, K. (2009). Disturbance accommodating control of floating offshore wind turbines. 47th AIAA Aerospace Sciences Meeting Including the New Horizons Forum and Aerospace Exposition. Orlando, Florida.
83. Namik, H., & Stol, K. (2010). Individual blade pitch control of floating offshore wind turbines. *Wind Energy*, *13*, 74–85. <https://doi.org/10.1002/we.332>.
84. Namik, H., Stol, K., & Jonkman, J. (2008). State-space control of tower motion for deepwater floating offshore wind turbines. 46th AIAA Aerospace Sciences Meeting and Exhibit.
85. Betti, G., Farina, M., Guagliardi, G. A., Marzorati, A., & Scattolini, R. (2014). Development of a control-oriented model of floating wind turbines. *IEEE Transactions on Control Systems Technology*, *22*(1), 69–82. <https://doi.org/10.1109/tcst.2013.2242073>.
86. Laugesen, R., & Hansen, A. M. (2015). Experimental study of the dynamic response of the DTU 10 MW wind turbine on a tension leg platform, Master's thesis, Department of Wind Energy, Technical University of Denmark, DK2800 Lyngby, 2015. Denmark DTU Wind Energy -0065, Master Thesis Report.
87. Madsen, F. J., Nielsen, T. R. L., Kim, T., Bredmose, H., Pegalajar-Jurado, A., Mikkelsen, R. F., et al. (2020). Experimental analysis of the scaled DTU10MW TLP floating wind turbine with different control strategies. *Renewable Energy*, *155*, 330–346. <https://doi.org/10.1016/j.renene.2020.03.145>.
88. Namik, H., & Stol, K. (2010). Individual blade pitch control of a floating offshore wind turbine on a tension leg platform. In: 48th AIAA Aerospace Sciences Meeting Including the New Horizons Forum and Aerospace Exposition. 2010.
89. Namik, H., & Stol, K. (2011). Performance analysis of individual blade pitch control of offshore wind turbines on two floating platforms. *Mechatronics*, *21*(4), 691–703. <https://doi.org/10.1016/j.mechatronics.2010.12.003>.
90. Zhang, M., Yang, H., & Xu, J. (2017). Numerical investigation of azimuth dependent smart rotor control on a large-scale offshore wind turbine. *Renewable Energy*, *105*, 248–256. <https://doi.org/10.1016/j.renene.2016.12.063>.
91. Zhang, M., Li, X., & Xu, J. (2019). Smart control of fatigue loads on a floating wind turbine with a tension-leg-platform. *Renewable Energy*, *134*, 745–756. <https://doi.org/10.1016/j.renene.2018.11.079>.
92. Larsen, T. J., & Hanson, T. D. (2007). A method to avoid negative damped low frequent tower vibrations for a floating, pitch controlled wind turbine. *Journal of Physics: Conference Series*, *75*. <https://doi.org/10.1088/1742-6596/75/1/012073>.
93. Ma, Z., Li, W., Ren, N., & Ou, J. (2017). The typhoon effect on the aerodynamic performance of a floating offshore wind turbine. *Journal of Ocean Engineering and Science*, *2*(4), 279–287. <https://doi.org/10.1016/j.joes.2017.09.004>.
94. Fischer, B. (2013). Reducing rotor speed variations of floating wind turbines by compensation of non-minimum phase zeros. *IET Renewable Power Generation*, *7*(4), 413–419. <https://doi.org/10.1049/iet-rpg.2012.0263>.

95. Wakui, T., Yoshimura, M., & Yokoyama, R. (2017). Multiple-feedback control of power output and platform pitching motion for a floating offshore wind turbine-generator system. *Energy*, *141*, 563–578. <https://doi.org/10.1016/j.energy.2017.09.100>.
96. Oh, Y., Kim, K., Kim, H., & Paek, I. (2015). Control algorithm of a floating wind turbine for reduction of tower loads and power fluctuation. *International Journal of Precision Engineering and Manufacturing*, *16*(9), 2041–2048. <https://doi.org/10.1007/s12541-015-0265-0>.
97. Zhu, H., Sueyoshi, M., Hu, C., & Yoshida, S. (2019). A study on a floating type shrouded wind turbine: Design, modeling and analysis. *Renewable Energy*, *134*, 1099–1113. <https://doi.org/10.1016/j.renene.2018.09.028>.
98. Yuan, Y., & Tang, J. (2017). Adaptive pitch control of wind turbine for load mitigation under structural uncertainties. *Renewable Energy*, *105*, 483–494. <https://doi.org/10.1016/j.renene.2016.12.068>.
99. Namik, H., & Stol, K. (2014). Individual blade pitch control of a spar-buoy floating wind turbine. *IEEE Transactions on Control Systems Technology*, *22*(1), 214–223. <https://doi.org/10.1109/tcst.2013.2251636>.
100. Chaaban, R., & Fritzen, C-P. (2014). Reducing blade fatigue and damping platform motions of floating wind turbines using model predictive control. Proceedings of the 9th International Conference on Structural Dynamics, EURO DYN 2014.
101. Raach, S., Schlipf, D., Sandner, F., Matha, D., & Cheng, P.W. (2014). Nonlinear model predictive control of floating wind turbines with individual pitch control. 2014 American Control Conference, Portland, OR, 2014, pp. 4434–4439, doi: 10.1109/ACC.2014.6858718.
102. Yang, F., Song, Q.-W., Wang, L., Zuo, S., & Li, S.-S. (2014). Wind and wave disturbances compensation to floating offshore wind turbine using improved individual pitch control based on fuzzy control strategy. *Abstract and Applied Analysis*, *2014*, 1–10. <https://doi.org/10.1155/2014/968384>.
103. Sarkar, S., Fitzgerald, B., & Basu, B. (2020). Individual blade pitch control of floating offshore wind turbines for load mitigation and power regulation. *IEEE Transactions on Control Systems Technology*. <https://doi.org/10.1109/tcst.2020.2975148>.
104. Yu, W., Lemmer, F., Bredmose, H., Borg, M., Pegalajar-Jurado, A., Mikkelsen, R. F., et al. (2017). The TripleSpar Campaign: Implementation and test of a blade pitch controller on a scaled floating wind turbine model. *Energy Procedia*, *137*, 323–338. <https://doi.org/10.1016/j.egypro.2017.10.357>.
105. Goupee, A. J., Kimball, R. W., & Dagher, H. J. (2017). Experimental observations of active blade pitch and generator control influence on floating wind turbine response. *Renewable Energy*, *104*, 9–19. <https://doi.org/10.1016/j.renene.2016.11.062>.
106. Kim, H. C., & Kim, M. H. (2018). The effects of blade-pitch control on the performance of semi-submersible-type floating offshore wind turbines. *Ocean Systems Engineering*, *8*, 79–99. <https://doi.org/10.12989/ose.2018.8.1.079>.
107. Lemmer, F., Yu, W., Schlipf, D., & Cheng, P. W. (2019). Robust gain scheduling baseline controller for floating offshore wind turbines. *Wind Energy*, *23*(1), 17–30. <https://doi.org/10.1002/we.2408>.
108. Han, C., & Nagamune, R. (2020). Platform position control of floating wind turbines using aerodynamic force. *Renewable Energy*, *151*, 896–907. <https://doi.org/10.1016/j.renene.2019.11.079>.

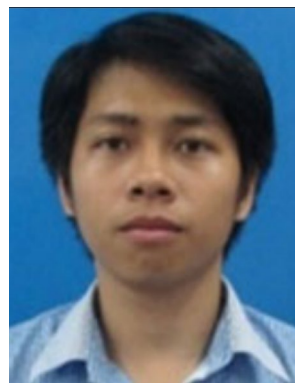
Publisher's Note Springer Nature remains neutral with regard to jurisdictional claims in published maps and institutional affiliations.



Kwang Ha received the B.S. in the Department of Automotive Engineering from Hanyang University in 1996, M.S. and Ph.D. in the Aerospace Engineering from the Georgia Institute of Technology in U.S.A. at 2005. His employment experience included the Groen Brothers Aviation, Caterpillar in U.S.A., Samsung Heavy Industry (SHI), Korea Aerospace Industry (KAI), and Fraunhofer Institute of Wind Energy System in Germany. He participated at the blade development of Hawk 5 Gyroplane at Groen Brothers Aviation and lead the 7MW Offshore Wind Turbine Development as a blade specialist at SHI. He also played a key role in Future Rotor Blade Concept Project at Fraunhofer IWES. He is currently working at Department of Floating Offshore Wind Energy System at the University of Ulsan as a Research Professor since Nov. 2019. His current researches are smart blade development for offshore wind turbine with composite structure tailoring and active materials.



Hoai Vu Anh Truong received the B.S. degree in mechanical engineering from Ho Chi Minh City University of Technology, Ho Chi Minh City, Vietnam, in 2015. He is currently a Ph.D. student of mechanical and automotive engineering, University of Ulsan, Ulsan, South Korea. His research interests include renewable energy, energy conversion systems, energy management for hybrid power source, advanced and intelligent controls for nonlinear system, impedance control and applications for robotic manipulator.



Tri Dung Dang received his B.S. degree in Mechatronics from Ho Chi Minh city University of Technology and Education, Viet Nam in 2013 and Ph.D. from University of Ulsan, Korea in 2019. He is currently working as postdoc researcher in Mechanical Department in University of Ulsan, Korea and Mechatronics Department in Ho Chi Minh city University of Technology and Education, Viet Nam. His research interests include energy management system, hydraulic system, PEM fuel cell vehicles, mechanism and control design for wave energy converter and wind turbine system.



Kyoung Kwan Ahn received the B.S. degree in the Department of Mechanical Engineering from Seoul National University in 1990, the M. Sc. degree in Mechanical Engineering from Korea Advanced Institute of Science and Technology (KAIST) in 1992 and the Ph.D. degree from Tokyo Institute of Technology in 1999, respectively. Since 2000, he has been with the School of Mechanical Engineering, University of Ulsan, where he is currently a Professor and the Director of the Fluid Power

Control and Machine Intelligence Laboratory. His main research interests include floating offshore wind turbine system control, fluid based

triboelectric nano generator, modeling and control of fluid power system, energy saving construction machine, hydraulic robot, and power transmission in the ocean energy. He is the author or coauthor of over 190 SCI(E) papers and four books in these areas. Dr. Ahn serves as an editor of International Journal of Control, Automation and Systems and editorial board of renewable energy, Korean fluid power and construction machine, Actuators and so on.